

# BE/APh 161: Physical Biology of the Cell

Justin Bois

Caltech

Winter, 2023



Donna and Benjamin M.  
Rosen Bioengineering Center

This document was prepared at Caltech with financial support from the Donna and Benjamin M. Rosen Bioengineering Center.

© 2023 Justin Bois, except for figures taken from literature sources.

This work, with the exception of figures from literature sources, is licensed under a [Creative Commons Attribution License CC-BY 4.0](#).

# 1 What is Physical Biology of the Cell?

You are enrolled in a class entitled *Physical Biology of the Cell*. An obvious first question to ask is, What is *Physical Biology of the Cell*? Perhaps this is best answered by considering an example.

## 1.1 Nucleosome wrapping

In eukaryotes, DNA is packaged in the nucleus in chromosomes. The chromosomes consist of condensed chromatin fibers. The chromatin fibers are made of packed nucleosomes. A nucleosome consists of an octameric histone and DNA wrapped around it. The histone is about 8 nm in diameter, and the DNA wraps around it almost twice. Approximately 147 base pairs of DNA are wrapped around this complex.

These facts about nucleosomes raise important questions. How does wrapping happen? How stable are the wrapped structures? What are the dynamics of the wrapped DNA on the histone (i.e., how does it “breathe”)? What do we need to know to be able to answer these questions?

- What is the energetic costs of bending the DNA?
- What is the interaction energy between the DNA and the nucleosome core complex?
- What is the magnitude of the electrostatic repulsion of the DNA?
- What is the geometry of the contacts?
- What other factors (such as reader-writer and code-reader complexes) may be in play *in vivo*?

These are all physical questions and they demand physical approaches.

Let’s talk about some of the approaches we could take. First, we could do a full all-atom molecular dynamics simulation. If we have a big enough computer, good enough force fields, and accurate enough structural information, we can just integrate equations of motion and get at the dynamics. This was done in Ettig, et al., *Biophys. J.*, **101**, 1999–2008, 2011. While impressive, the limits of computation mean that we can only simulate 10s of nanoseconds. Furthermore, electrostatics are hard to treat.

As an alternative approach, we could do a simulation in which the nucleotides and amino acids in the proteins are coarsened into beads that interact with each other via harmonic and Morse potentials. This was done in Voltz, et al., *Biophys. J.*, **102**, 849–858, 2012. They found some long-lived DNA detachments and discovered that the so-called H3 tail of the histone was an important player in these detachments.

### 1.1.1 A coarsened approach to DNA bending

While these computational approaches are useful and yield insight, we might want to zoom out some more to get a broader picture of nucleosome construction. Let’s treat the DNA as a **semiflexible filament**. That is, it is an elastic rod that can bend, but resists doing so.<sup>1</sup> With this coarsened treatment, we can use some of the knowledge about elastic rods that structural engineers have known for a long

---

<sup>1</sup>We will talk about semiflexible filaments in much greater depth later in the course.

time. Specifically, the bending energy of the segment of DNA of length  $\ell$  around the histone is given by

$$\frac{E_{\text{bend}}}{\ell} = \frac{1}{2} EI C^2. \quad (1.1)$$

Here,  $E$  is the Young's modulus,  $I$  is the moment of inertia, and  $C$  is curvature. We will discuss these terms in depth later in the course, but for now we mention that a larger Young's modulus means that the rod is harder to bend, and the moment of inertia is a function of the cross-sectional geometry of the filament. The curvature is the inverse of the radius of curvature,  $R$ . We often define the **flexural rigidity**  $K$  as  $K = EI$ . Then, we have

$$\frac{E_{\text{bend}}}{\ell} = \frac{1}{2} \frac{K}{R^2}. \quad (1.2)$$

What is the flexural rigidity of DNA? This is sometimes easier thought of in terms of a **persistence length**. The persistence length,  $\xi_p$ , can be defined as the length scale where the bending energy is of the same magnitude as the thermal energy  $kT$ .

$$E_{\text{bend}} \approx kT = \frac{K}{\xi_p}, \quad (1.3)$$

which gives  $K = \xi_p kT$ . So,

$$\frac{E_{\text{bend}}}{\ell} = \frac{1}{2} \frac{\xi_p kT}{R^2}. \quad (1.4)$$

So, we now have a way to estimate the bending energy. We only need to know the persistence length of DNA, which was measured by elegant single molecule experiments in the early 90s to be about 50 nm. The base stack height in DNA, known from crystal structures, is 0.34 nm. Since 127 base pairs are bent around the histone (147 base pairs go around the histone in total, but the ten base pairs on each end are straight), we have 43 nm of bent wrapped DNA. The radius of curvature is  $R \approx 4$  nm, since the histone core is about 8 nm in diameter. Finally, the thermal energy  $kT$  is about 4.1 pN-nm (piconewton-nanometers) at physiological temperatures. We have all the pieces we need.

$$E_{\text{bend}} \approx \frac{\ell}{2} \frac{\xi_p kT}{R^2} \approx \frac{43 \text{ nm}}{2} \frac{50 \text{ nm} \cdot 4.1 \text{ pN-nm}}{(4 \text{ nm})^2} \approx 275 \text{ pN-nm} \approx 65 kT. \quad (1.5)$$

So, we already know that the binding energy between the histone and the DNA filament must be more than  $65 kT$ , or 275 pN-nm.

### 1.1.2 The energetics of DNA-histone interactions

From crystal structures, we know that the DNA contacts the histone in the minor groove when it faces inwards. Thus, we have histone-DNA contact every helical twist, or about every 10 base pairs. There are then 14 total contacts. Assuming they are all about the same, we have 14 times the interaction energy of a single contact contributing to the DNA-histone binding energy.

Polach and Widom did an ingenious experiment to measure this binding energy. They wrapped sequences of DNA around a histone and then put the nucleosome complexes in a solution with restriction enzymes that cleave the DNA at a specific point if that point is not bound to the histone. They then looked at the probability of a segment of DNA being unwound, which is possible because

this probability is proportional the rate of cleavage. This, in turn, is proportional to  $e^{-nE_{\text{net}}/kT}$ , where  $E_{\text{net}}$  is the free energy of binding of one site of the DNA to the histone and  $n$  is the number of points that need to be unbound to unwind the DNA. Note that this is the *net* binding energy that includes all energetics, including the DNA bending energy. They found that the rate of cleavage for cut points in the middle of the wrapped DNA were about 4 or 5 orders of magnitude greater than for cut points at the ends. So, we can compute the free energy of binding a single site, knowing that a single site becomes unbound for cleavage at the end of the wrapped DNA and seven sites become unbound for a site at the center.

$$\frac{e^{-E_{\text{net}}/kT}}{e^{-7E_{\text{net}}/kT}} = 10^{-4} \text{ or } 10^{-5}. \quad (1.6)$$

This gives  $E_{\text{net}} \approx 1.5\text{--}2 kT \approx 6\text{--}8 \text{ pN}\cdot\text{nm}$ . Multiplying this by the 14 sites gives the total binding energy as

$$E_{\text{tot}} \approx 28 kT \approx 112 \text{ pN}\cdot\text{nm}. \quad (1.7)$$

Therefore, the binding energy, exclusive of DNA bending is about  $65 kT + 28 kT \approx 90 kT$ , or about  $6 kT$  per binding site. So, more than 2/3 of the binding energy is spent just bending the DNA around the histone. Furthermore, the total binding energy is only  $6 kT$  per site, so thermal fluctuations can result in significant “breathing” of the complex.

## 1.2 This is Physical Biology of the Cell

What we just did is physical biology of the cell. We took a biological problem and took a quantitative, physical approach to solving it. We build a simple, treatable model that is sufficient for our question (a rigid beam wrapped around a cylinder with point-contacts). The model allows use to measure parameters.

This approach allows us to:

- Define and measure parameters.
- Generate falsifiable predictions.
- Bridge concepts across length and time scales.
- Deal with complexity. We choose appropriate models for the desired level of detail.
- Illuminate life’s constraints. Life, like everything, is bound by the laws of physics.
- Make synthetic biology possible. The ability to make predictions about how systems will behave, as physics can do, enables *engineering*.

## 1.3 What Physical Biology of the Cell is not

What will we *not* be doing in this class?

- Biology with some math. All too often, a biologist will do some great work and then throw in some math because it is sexy and will get their paper in a better journal. We are only interested in learning about biology if and when physical models are necessary.

- Biology-inspired physics. *Physical* questions often arise from biology. These are often very interesting to physicists and useful for exposing undiscovered physical principles, but do not explain biological phenomena. These are great studies, but not what we will do here. We want to learn about *biology*.
- Model-making for understood systems. This is kind of like “biology with some math.” We do not need to invent models unless we are trying to gain a *deeper* understanding. Making a model that happens to match already measured and understood results is superfluous (and often part of research teams hunting for a more prestigious journal for their paper).

## 2 Principles of estimation

As we discussed in the first lecture, one of our main aims in this course is to develop a sense of biological numeracy. A great way to do this is by performing estimates and back-of-the-envelope calculations about cells. Indeed, detail can often get in the way. For example, I may ask you if you prefer to fly or drive from Pasadena to San Francisco. You can hire a rideshare to Burbank, take a Southwest flight to Oakland, and then take the BART to San Francisco. The rideshare takes about 20 minutes, the flight about an hour, the BART takes about 20 minutes, and you have about an hour at the airport in Burbank and about 30 minutes at Oakland to get to the BART. In total, this is about 2.5 hours. Driving takes 5.5 hours without traffic, so you will choose to fly. Now, if we did this calculation trying to estimate how many minutes it takes for the Lyft driver to come, precisely how many minutes in baggage claim, etc., the calculation becomes cumbersome. Maybe more accurate, but you will still get more or less 2.5 hours to fly to San Francisco. It's easier, and more intuitive, to ignore all the little ins and outs. You end up with good intuition on how long things take nonetheless.

### 2.1 How many ribosomes in an *E. coli* cell?

Let's start learning about bacterial cells by performing a simple estimate: how many ribosomes are there in a single *E. coli* cell? We will take as given two pieces of data, a microscope image of an *E. coli* cell and an image of the growth rate, shown in Fig. 1, taken from *PBoC2* Fig. 3.8.

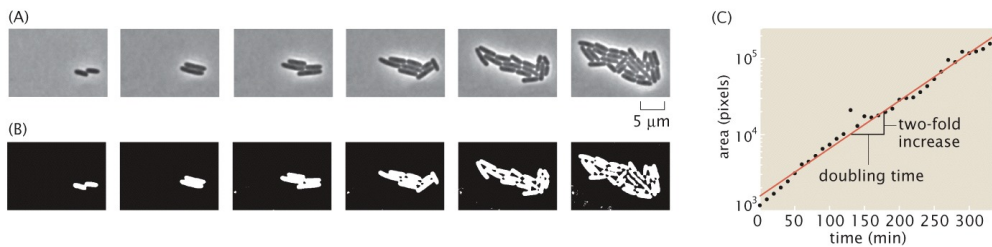


Figure 3.8 Physical Biology of the Cell, 2ed. (© Garland Science 2013)

Figure 1: A) Frames from a time lapse movie of bacterial growth with thresholding-based segmentation. B) A plot of the corresponding area of bacteria in the image as a function of time.

From the microscope image, we see that a single *E. coli* cell is about two microns long and one micron wide. From the growth curve, we see that the doubling time of *E. coli* in these conditions is about 45 minutes, or about 3000 seconds. Notice that I roughly estimated these values. 3000 seconds is 50 minutes, not 45, but we do not get bogged down in small differences like that.

At face this seems like a daunting task, estimating the number of ribosomes from only an image and a growth curve. But it is not so daunting if we divide the question up into smaller, more tractable (and less intimidating) questions. We can make a series of guesses to get us from what we know (the size of a cell and growth rate) to something else we *want to know* (the number of ribosomes).

Cell size (known).

1. **Estimate:** Cell density → Cell mass.
2. **Estimate:** Dry weight fraction → Cell dry mass.

3. **Estimate:** Fraction of dry mass that is protein → Cell protein mass.
4. **Known:** Cell division rate → Protein production rate by mass.
5. **Estimate:** Mass of amino acid → Protein production rate in units of AAs incorporated per second.
6. **Estimate:** Rate of ribosome function → Number of ribosomes.

Let's start estimating!

**1.** What is the cell density? A reasonable estimate is that it is close to that of water, which is 1 g/mL. We don't know the density, but we can **lie skillfully** to guess that it is the same as water. This is not a bad guess. To get the mass of a cell, we use our knowledge about its size. The volume of an *E. coli* cell is

$$V \approx \pi(1/2 \text{ }\mu\text{m})^2 \times 2 \text{ }\mu\text{m} \approx 1 \text{ }\mu\text{m}^3 = 1 \text{ fL.} \quad (2.1)$$

Note that the volume is closer to  $1.5 \text{ }\mu\text{m}^3$ , but for our rough estimates, we'll keep our numbers clear, and approximate this as one cubic micron, or one femtoliter. This is a nice number to keep around. **The volume of a single *E. coli* cell is about one femtoliter.**

Now that we have the volume and density, we compute the mass to be  $10^{-12}$  grams, or one picogram, another useful number to keep in your head.

**2.** Now that we have the mass of the cell, how much of that is water? This is a bit tricky. You may have heard that your body is 80% water from popular lore. That's not actually that far off, and you could go ahead with your estimates taking that the *E. coli* cell is about 20% dry mass, or 0.2 pg.

Another option I considered it to recall my training from chemistry classes where I looked at closest packing of spheres. I remember that the fractional void volume of closest packed spheres is  $1 - \pi/\sqrt{18}$ , or about 25%. (I have no idea why that stuck in my head.) That's for closest packed spheres, but things need to diffuse around in the cell, so the void volume is probably more than that, say two or three times that. So, we'll say that the solid material takes about one-third of the total cell volume. 33% is not too different from 20%, and we'll use 33% going forward.

This tactic in our educated guesswork, where we use any knowledge that happens to be in our head, is called **guerrilla warfare**.

**3.** How much of this dry mass is actually protein? In a cell, proteins *do* most things and have longer lifetimes than, say, RNAs. So, let's guess that about half of the dry mass is protein, so about 1/6 of the total cellular mass is protein, or about 15%. This gives a protein mass of 0.15 pg.

You might think that this is nuts. I'm making guesses seemingly off the top of my head. But this exposes an important principle of educated guess work: **Fear not!**, lest you be paralyzed. Sometimes you need to make these guesses to move forward. Just do it, and **cross-check** later.

**4.** From the plot of the growth curve, we estimated that *E. coli* under those conditions divided every 45 minutes. Thus, each cell needs to produce 0.15 pg of protein every 45 minutes. Forty-five minutes is about 3000 seconds, so the bacterium needs to produce  $5 \times 10^{-5}$  pg of protein every second.

For convenience, let's work in mass units of Daltons. We have

$$5 \times 10^{-5} \text{ pg/s} \times \frac{1 \text{ g}}{10^{12} \text{ pg}} \times \frac{6 \times 10^{23} \text{ Da}}{1 \text{ g}} \approx 3 \times 10^7 \text{ Da/s.} \quad (2.2)$$

**5.** How many amino acids are there in  $3 \times 10^7$  Daltons worth of protein? A typical amino acid has a nitrogen, two carbons, two oxygens, and a side chain. The nitrogen contributes 14 Daltons, the carbons 24, and the oxygens 32, for a total of 70 Daltons, exclusive of hydrogens and side chains. We'll estimate that the side chains, on average, bring the mass of each amino acid up to about 100 Da. So, the bacterium incorporates about  $3 \times 10^5$  amino acids into proteins per second.

**6.** We are now left to estimate the rate at which ribosomes function. This is a hard one to guess. If we guess it to be too slow, the cell will fill up with ribosomes, which sets a hard lower bound on this guess. To make this guess, I will use the fact that diffusion-limited chemical reactions between proteins tend to proceed with rate constants around 100 to 1000  $\text{s}^{-1}$ . There are several reactions that have to happen to add an amino acid to a protein, including diffusion of the tRNA into the pocket of the ribosome, formation of covalent bond, vacation of tRNA, moving the DNA strand forward etc. These are also big complexes, so I will estimate the rate to be an order of magnitude slower, about 10 AAs per second.

So, if the bacterium incorporates  $3 \times 10^5$  amino acids into protein per second, and each ribosome does this at a rate of about 10 amino acids per second, there are about 30,000 ribosomes in an *E. coli* cell. And we have arrived at the estimate we sought.

## 2.2 Principles of estimation

We have performed an estimate of the number of ribosomes in an *E. coli* cell. In doing so, we have navigated some seemingly dangerous waters, but in the end emerged with an estimate quite close to the reported value.

As you do more estimates, there are some principles of estimation to keep in mind.

**1. Fear not!**

It is all too easy to be paralyzed and be afraid to make an estimate because it is too crude or you are not sure enough. *Just do it!* You can always come back later and refine.

**2. Divide and conquer.**

We just saw that it is easier to break the problem down into smaller, easier estimates. This is a key strategy for tackling what might be at first glance a really tough quantity to estimate.

**3. Talk to your gut.**

When you are making estimates, ask yourself, “Does this feel right?”. Somehow your collection of experiences in your life can help you have a good gut feel for things.

**4. Lie skillfully.**

Do you know the density of *E. coli*? Probably not. But you can lie and say it's the same as water. And this is a good lie, because it's not far from the truth, and you know it's not far from the truth. This is a good, skillful lie. Such lying will help you with your estimates.

**5. Guerrilla warfare.**

Use everything available to you!

#### 6. Cross-check.

After making an estimate, try making it using another divide-and-conquer strategy. If the two estimates do not match, it is time to check what may have messed things up. Such inconsistencies are a great way to find flawed (and good) logic.

### 2.3 More practice

It's common to have questions pop in your mind when making estimates. Now that you have in your mind the number of ribosomes in an *E. coli* cell, try approaching these questions.

1. What fraction of the protein material in an *E. coli* cell is made out of ribosomes?
2. How many mRNA transcripts are there in an *E. coli* cell at any given time? With this number, how many mRNA molecules are there per gene?
3. How does the mass of mRNA in an *E. coli* cell compare to that of DNA?
4. How does the mass of ribosomal RNA compare to that of mRNA and DNA?

There are many ways to approach these practice problems. Here are the approaches I took.

**What fraction of the protein material in an *E. coli* cell is made out of ribosomes?** A typical protein is about 300 amino acids, giving a mass of about  $3 \times 10^4$  Da. Ribosomes contain about 50 proteins, so their mass is about  $10^6$  Da. (The real value is about three times this.) With 30,000 ribosomes, this amounts to  $3 \times 10^{10}$  Da in ribosome protein mass. We already worked out that the total protein mass is about 0.15 pg, which is about  $10^{11}$  Da. By our estimate, then, a third of protein in an *E. coli* cell are ribosomes. If we take the actually molecular mass of ribosomes, we get that almost all protein is ribosomes. So, the cell is basically just a ribosome factory during optimal growth conditions!

#### How many mRNA transcripts are there in an *E. coli* cell at any given time?

We can approach this problem from above and from below. As an upper bound, we can imaging that each mRNA molecules is a single ribosome attached to it. This would mean we have 30,000 mRNA molecules as an upper bound. As a lower bound, we can imagine that each mRNA molecule is completely covered in ribosomes. To perform the calculation, then, we need to know the width of a ribosome and the length of an mRNA transcript.

A ribosome has a “volume” of about 50 proteins, so it has a diameter of about  $\sqrt[3]{50} \approx 4$  proteins. Proteins are typically a few nanometers across, so a ribosome is about 12 nanometers across. At least half of the ribosome is rRNA, which we have not yet considered so we'll double this number to about 20 nm.

To compute the length of an mRNA transcript, we note that the stack height of RNA

is about 0.4 nm. If a typical protein has 300 amino acids, this means there are about 900 mRNA bases, for a total length of about 500 nm.

So, if the ribosomes completely cover the mRNA, we have a total length of  $30,000 \times 20 \text{ nm} = 600,000 \text{ nm}$  worth of mRNA. This amounts to about 1000 mRNA molecules. So, there is somewhere between  $10^3$  and  $10^4$  mRNA molecules. We can take the geometric mean to get that we have about 3,000 mRNA molecules in an *E. coli* cell. [BNID 100064](#) says that there are about 1400, closer to the lower bound, suggesting that the mRNA molecules are densely decorated with ribosomes, which is what we would expect for a rapidly (efficiently) growing cell.

Since *E. coli* has about 5000 genes, there are only about 0.2 copies of mRNA per gene in *E. coli*.

### **How does the mass of mRNA in an *E. coli* cell compare to that of DNA?**

RNA and DNA have similar molecular masses per base, with mRNA being a bit heavier. We'll take them to have the same per base mass. The genome is about 4.6 million base pairs, or about 10 million DNA bases. If we have 3,000 mRNA molecules, each with about 900 bases, we have about 3 million RNA bases. So, the mass of DNA is about three times than of mRNA. Here we have neglected multiple copies of the genome due to multiple replication forks.

### **How does the mass of ribosomal RNA compare to that of mRNA and DNA?**

If we compare total RNA mass to DNA mass, we need to consider also the rRNA. Each ribosome is about half rRNA and has a molecular mass of about  $3 \times 10^6 \text{ Da}$ . So, there is about  $10^6 \text{ Da}$  of rRNA in a ribosome, giving about  $3 \times 10^{10} \text{ Da}$  of rRNA in the 30,000 ribosomes in the cell. Each base is about 300 Da, giving a total of about  $10^8$  bases worth of rRNA. This is a couple orders of magnitude bigger than the amount of mRNA in the cell, and an order of magnitude bigger than the DNA mass.

## 3 Mathematizing cartoons

The word “model” in biology has many meanings. There are three main ones, so far as I can tell.

**Cartoon models.** These models are the typical cartoons or qualitative verbal descriptions we see in text books or in discussion sections of biological papers. They are a sketch of what we think might be happening in a system of interest, but they do not provide quantifiable predictions.

**Physical models.** These models give quantifiable predictions that must be true if a hypothesis (which is often sketched as a *cartoon*) is true. Sometimes hard work and deep thought are needed to generate quantitative predictions. This often requires “mathematizing” the cartoon. This is how a *physical model* is derived from a *cartoon*. Oftentimes when biological physicists refer to a “model,” they are talking about a physical model.

**Generative statistical models.** A generative statistical model specifies how we expect measured data to be generated using the language of probability. Specifically, it describes how the measurements are expected to vary from the *physical model* because of measurement noise and other sources of variation.

In this class, we will be working mainly on physical models. The connection of these models to their respective cartoons is of paramount importance. We often think of biological systems in terms of the cartoons, and we need to understand what parameters and what quantifiable measurements result from the cartoons. Perhaps most importantly, we need to know what falsifiable hypotheses follow from a cartoon.

In this lecture, we will learn how to go from a cartoon to a physical model. The authors of *PBoC2* call this “mathematizing a cartoon.” We will do this mainly by example, and you will get a chance to practice other examples in the homework throughout the course.

There is a [companion Jupyter notebook to this lecture](#) that has the details of the numerical calculations.

### 3.1 Flagellar growth and length control in *Chlamydomonas reinhardtii*

We will cut our physical modeling teeth on a beautiful system: the growth of flagella in *Chlamydomonas reinhardtii*. *Chlamydomonas* has two flagella of the same length that it uses to swim. These flagella are constructed from microtubules arranged in a fascinating structure called an *axoneme*. The flagella are thought to be built by motor proteins that shuttle tubulin dimers from the bulk cytoplasm along the microtubules of the flagella to the ends, where they are incorporated into the microtubules. At the same time, there is spontaneous disassembly at the tip of the microtubules.

#### 3.1.1 Our first try: a simple model

As a first try at modeling assembly, we assume the motors deliver tubulin to the tip of the flagellum at a constant rate  $\beta$  and that the microtubules depolymerize at a constant rate  $\alpha$ . Then, the length

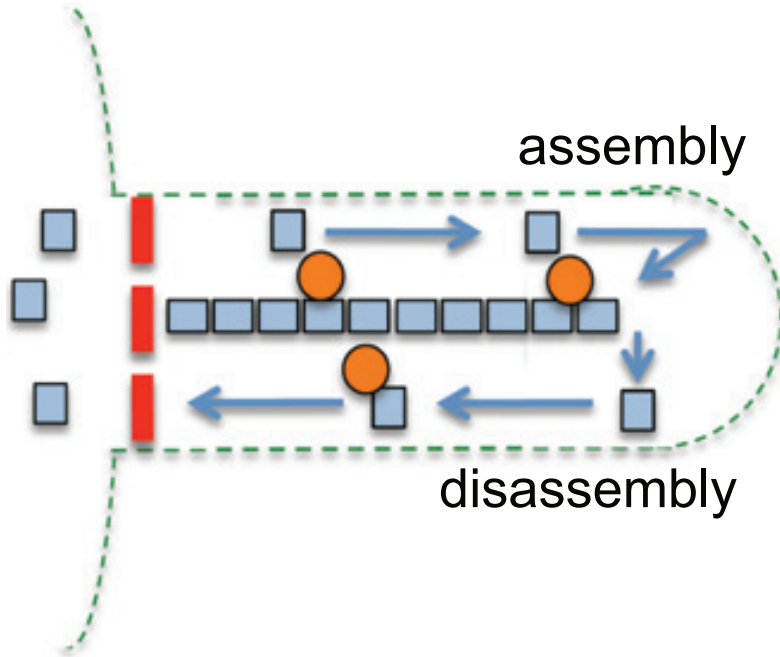


Figure 2: A cartoon sketch of the balance point model. Motor proteins (Orange circles) transport tubulin (blue squares) and other necessary axoneme growth elements to the distal tip of the flagellum. There is spontaneous disassembly at the tip. Figure taken from Avasthi and Marshall, *Differentiation*, 83, S30-S42, 2012.

of the flagellum, measured in units of number of added tubulin dimers is described by the differential equation

$$\frac{d\ell}{dt} = \beta - \alpha. \quad (3.1)$$

The solution to this differential equation is

$$\ell(t) = \ell_0 + (\beta - \alpha)t. \quad (3.2)$$

This model is obviously flawed because the flagellum would grow without bound with  $\beta > \alpha$  and would shrink to nothing with  $\beta < \alpha$ . So, by mathematizing the model, we have immediately exposed a certain model as unfeasible.

### 3.1.2 A refinement: the “balance point model”

Marshall and Rosenbaum (2001) proposed a refinement on our first simple model. They noted that there are a constant number of motor proteins present in the flagellum as it grows. So, the density of motors is greater early on in the growth (when it is short) and more sparse later on (when it is long). We might estimate that the rate of delivery of material to the tip of the microtubule is then proportional to the motor density,  $\rho = N_{IFT}/\ell$ , where  $N_{IFT}$  is the constant number of particles involved in intraflagellar transport (IFT). Now, the dynamics read

$$\frac{d\ell}{dt} = \beta/\ell - \alpha, \quad (3.3)$$

where we have wrapped constants into the parameter  $\beta$  such that  $\beta \propto N_{\text{IFT}}$ . Now, we have a unique steady state length of  $\beta/\alpha$ . Let's look at this equation and see what it tells us about the dynamics of microtubule growth.

It is often good practice, especially when doing a numerical solution, to **nondimensionalize** the equations first. This limits the number of parameters we need to vary. For the balance point model, we have two parameters,  $\beta$  and  $\alpha$ , which have units of length squared per time and length per time, respectively. We can then construct a characteristic length scale  $\beta/\alpha$  and a characteristic time scale  $\beta/\alpha^2$ . We define dimensionless length  $\tilde{\ell}$  via  $\ell = \beta\tilde{\ell}/\alpha$  and dimensionless time  $\tilde{t}$  via  $t = \beta\tilde{t}/\alpha^2$ . Substituting these expressions into the balance point model gives

$$\frac{d\tilde{\ell}}{d\tilde{t}} = \tilde{\ell}^{-1} - 1. \quad (3.4)$$

It's useful to analyze the differential equation to get some qualitative features. We have already established a unique steady state of  $\tilde{\ell} = 1$ . Because the derivative positive for all  $\tilde{\ell} < 1$  and negative for all  $\tilde{\ell} > 1$ , the flagellar length proceeds monotonically toward the steady state. We can rewrite the differential equation in terms of the distance from the steady state,  $\varepsilon = 1 - \tilde{\ell}$ . Making this substitution gives

$$\frac{d\varepsilon}{d\tilde{t}} = -\frac{\varepsilon}{1-\varepsilon}. \quad (3.5)$$

The flagellum approaches the steady state slowly<sup>2</sup>, with the distance from the steady state,  $\varepsilon$ , decreasing like  $\varepsilon/(1-\varepsilon)$ . At short times, we get incredibly fast growth. This is unphysical, since our assumption of constant IFT particle concentration breaks down as the flagellar length goes to zero (as this would result in infinite IFT particle concentration). This is a common feature of mathematical models. They have a region of validity, in this case for  $\ell$  not too close to zero.

The solution to the differential equation results in either a transcendental equation for  $\tilde{\ell}$  or use of the Lambert-W function. Either way, the solution is ugly and not terribly informative. I am generally of the opinion that solving differential equations is only useful if the solution provides some insight or enables taking of some limit. When the only interpretable result we can get out of an analytical solution is a plot, we are equally well-served by solving the differential equation numerically.

### 3.1.3 The balance point model and experiment

Engel, Ludington, and Marshall (Engel, et al., *J. Cell Biol.*, **187**, 81-89, 2009) measured the growth of flagella after pH shock, which eliminates the flagella. I digitized their result from Fig. 1 of that paper and performed a nonlinear regression using the balance point model. The details of the calculation can be found in the [companion Jupyter notebook to this lecture](#). The results are shown in Fig. 3. This provides evidence that the balance point model might be describing microtubule growth dynamics.

### 3.1.4 Testing the balance point model

The balance point model, as we have formulated it, assumes each flagellum is independent of all others. Therefore, if we sever one flagellum and watch it grow back, the other flagellum should be

---

<sup>2</sup>This is slower than exponential, since the Taylor series of  $\varepsilon/(1-\varepsilon)$  is  $\sum_{n=1}^{\infty} \varepsilon^n$ .

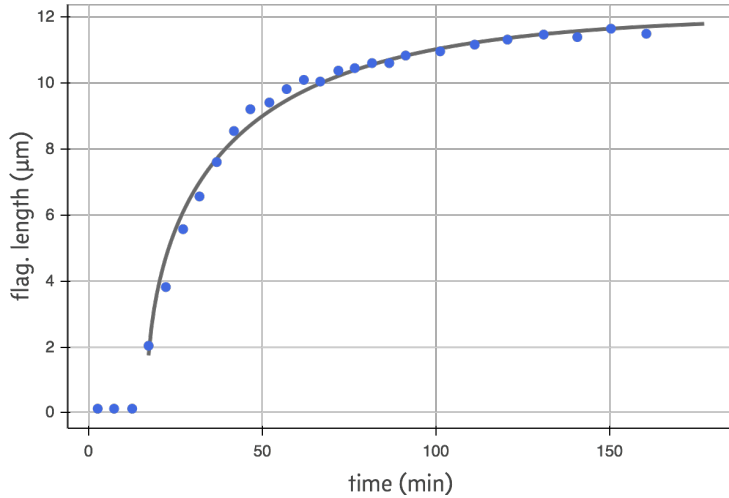


Figure 3: Curve fit of the balance point model to the data digitized from the Engel, et al., paper. The best fit parameters as  $\alpha = 0.23 \mu\text{m}/\text{s}$  and  $\beta = 2.74 \mu\text{m}^2/\text{s}$ .

unaffected under the model. Ludington and coworkers devised a clever experiment in which they trapped individual *Chlamydomonas* cells using a microfluidic device and then used a laser to sever one of the flagella (see Fig. 4).

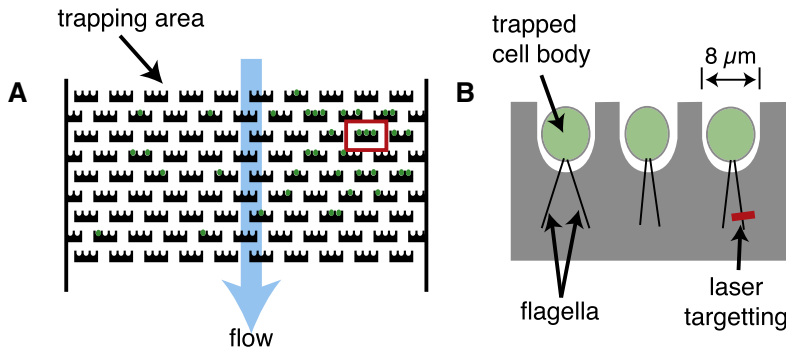


Figure 4: A) Schematic of microfluidic device for trapping of individual *Chlamydomonas* cells. B) Trapped cells and laser ablation setup. Figure take from Ludington, et al., *Curr. Biol.*, **22**, 2173–2179, 2012.

Ludington and coworkers instead saw that the length of the non-severed microtubule shrank while the other grew, as shown in Fig. 5. This means that the two are not independent.

### 3.1.5 Updating the balance point model

There is clearly some connection between the two flagella. What might this connection be? One hypothesis is that the two flagella share a cytoplasmic pool of tubulin. Specifically, let  $n$  be the number of axoneme components (which we'll just call precursor for brevity) in the cytoplasm available for

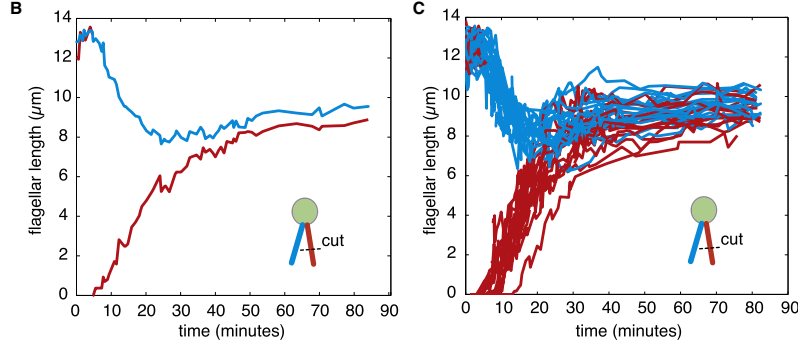


Figure 5: B) Results from a single laser ablation-regrowth experiment. C) The response of 20 cells who had flagella ablated simultaneously in the same microfluidic chamber. Figure taken from Ludington, et al., *Curr. Biol.*, **22**, 2173–2179, 2012.

incorporation into the flagella. We will again use units of  $\mu\text{m}$  for  $n$ . Then the amount of precursor that an IFT train at the base of the flagellum can pick up is a function of  $n$ . This is expressed in the cartoon in Fig. 6

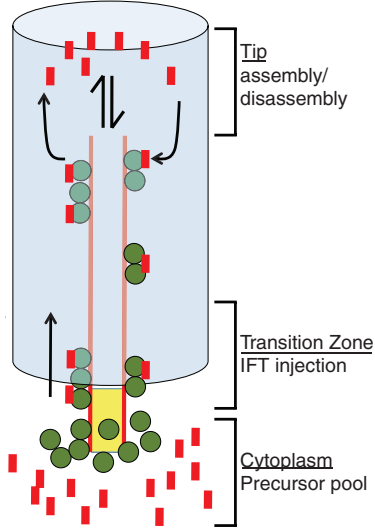


Figure 6: An updated balance point model where the cytoplasm contains a pool of axoneme components to be transported by motor proteins to the tip. Figure taken from Chan and Marshall, *Science*, **337**, 1186–1189, 2012.

We will now write down an updated balance point model for two flagella that share the same (conserved) cytoplasmic pool of precursor. We use units of concentration that are consistent with flagellar length. That is, concentrations are units of  $\mu\text{m}$  per volume. Let  $\ell_1$  and  $\ell_2$  be the lengths of the respective microtubules. Let the anterograde IFT train speed be  $v_a$  and the retrograde IFT train speed by  $v_r$ . The time it takes an IFT train to reach the tip is  $\ell_i/v_a$ , and the amount of time it takes the disassembled particles to reach the base is  $\ell_i/v_r$ . We will approximate the rate of pickup of precursor at the base as a linear function of the train density and the cytoplasmic concentration. (Remember that the density of transporters goes like  $1/\ell_i$ .) Then, we can write delayed differential

equations describing the length of the flagella.

$$\frac{d\ell_1}{dt} = \beta \frac{n(t - \ell_1/v_a)}{\ell_1} - \alpha, \quad (3.6)$$

$$\frac{d\ell_2}{dt} = \beta \frac{n(t - \ell_2/v_a)}{\ell_2} - \alpha. \quad (3.7)$$

We can write a differential equation for removal and delivery from the cytoplasm.

$$\frac{dn}{dt} = -\beta n \left( \frac{1}{\ell_1} + \frac{1}{\ell_2} \right) + 2\alpha. \quad (3.8)$$

Here,  $V$  is the volume in which the precursor particles reside. (This may be the entire, well mixed cell, or some pocket in the cytoplasm where the precursors are localized.) Note that here,  $\beta$  has a different meaning than before. Its units are now  $\mu\text{m}/\text{s}$ . Note also that even though tubulin that is disassembled from the tip takes a time  $\ell_i/v_r$  to return to the cytoplasm, there is no explicit time delay in the  $n$  dynamics because this is a constant process.

We also have conservation of total flagellar material.

$$n_{\text{tot}} = n + \ell_1 + \ell_2. \quad (3.9)$$

These equations allow us to compute the steady state. From the dynamics of  $\ell_1$  and  $\ell_2$ , it is clear that  $\ell_1 = \ell_2 = \beta n/\alpha$  at steady state. Inserting this expression into the conservation law gives the steady state.

$$n = \frac{\alpha n_{\text{tot}}}{\alpha + 2\beta}. \quad (3.10)$$

### 3.1.6 Nondimensionalization of the updated balance point model

To nondimensionalize, we need to choose units for  $\ell_1$  and  $\ell_2$ , which we'll call  $\ell_0$ , units for time,  $\tau$ , and units for the cytoplasmic number of precursors,  $n_0$ . We define  $\ell_1 = \ell_0 \tilde{\ell}_1$ ,  $\ell_2 = \ell_0 \tilde{\ell}_2$ ,  $t = \tau \tilde{t}$ , and  $n = n_0 \tilde{n}$ . Then, the dynamical equations are

$$\frac{d\tilde{\ell}_1}{d\tilde{t}} = \frac{\beta n_0 \tau}{\ell_0^2} \frac{\tilde{n} \left( \tilde{t} - \frac{\ell_0}{\tau v_a} \tilde{\ell}_1 \right)}{\tilde{\ell}_1} - \frac{\alpha \tau}{\ell_0}, \quad (3.11)$$

$$\frac{d\tilde{\ell}_2}{d\tilde{t}} = \frac{\beta n_0 \tau}{\ell_0^2} \frac{\tilde{n} \left( \tilde{t} - \frac{\ell_0}{\tau v_a} \tilde{\ell}_2 \right)}{\tilde{\ell}_2} - \frac{\alpha \tau}{\ell_0}, \quad (3.12)$$

$$\frac{d\tilde{n}}{d\tilde{t}} = -\frac{\beta \tau}{\ell_0} \tilde{n}(\tilde{t}) \left( \frac{1}{\tilde{\ell}_1} + \frac{1}{\tilde{\ell}_2} \right) + \frac{2\alpha \tau}{n_0}. \quad (3.13)$$

To eliminate parameters, we choose  $\tau = \ell_0/\alpha$  and  $\ell_0/n_0 = \beta/\alpha \equiv \gamma$ . The dimensionless equations then become

$$\frac{d\tilde{\ell}_1}{d\tilde{t}} = \frac{\tilde{n}(\tilde{t} - \tilde{\ell}_1/u)}{\tilde{\ell}_1} - 1, \quad (3.14)$$

$$\frac{d\tilde{\ell}_2}{d\tilde{t}} = \frac{\tilde{n}(\tilde{t} - \tilde{\ell}_2/u)}{\tilde{\ell}_2} - 1, \quad (3.15)$$

$$\frac{1}{\gamma} \frac{d\tilde{n}}{d\tilde{t}} = -\tilde{n}(\tilde{t}) \left( \frac{1}{\ell_1} + \frac{1}{\ell_2} \right) + 2, \quad (3.16)$$

where we have defined  $u \equiv v_a/\alpha$ . We see that the dynamical equations depend only on two parameters: the ratio of pick-up rate of precursor to shedding rate from the tip and the ratio of transport to the tip and shedding rate. To connect to real units, we have to specify one of  $\ell_0$ ,  $n_0$ , or  $\tau$  in terms of  $\alpha$ ,  $\beta$ ,  $n_{\text{tot}}$ , and  $v_a$ , the physical parameters of the system. We could specify  $n_0 = n_{\text{tot}}$ , giving  $\ell_0 = \gamma n_{\text{tot}}$  and  $\tau = \beta n_{\text{tot}}/\alpha^2$ . We note that we always have to make sure that we set initial conditions such that  $\tilde{n} + \gamma(\tilde{\ell}_1 + \tilde{\ell}_2) < 1$  to obey conservation of mass. Any difference of this sum from unity is indicative of precursor material that is in transit in the flagellum, so this sum should be close to unity.

### 3.1.7 Adjusted balance point model and experiments.

We can again fit the adjusted balance point model to growth data from the pH shock experiment. The result is shown in Fig. 7. We again have good agreement with the growth curve.

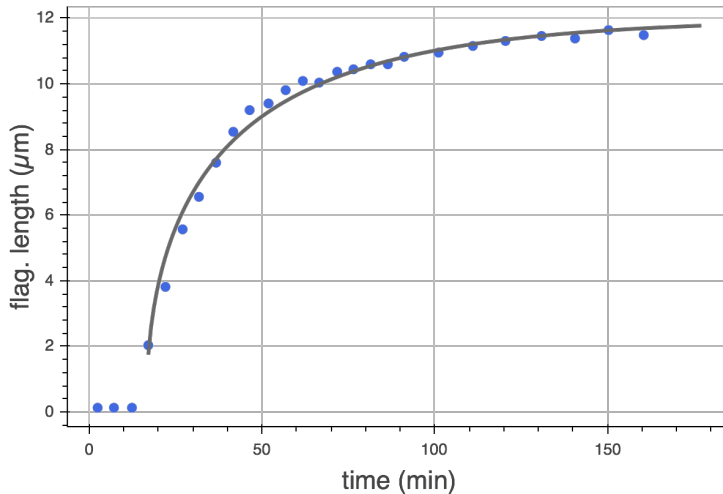


Figure 7: Fit of growth from the pH shock experiment using the adjusted balance point model. The best fit parameters are  $\alpha = 0.073 \mu\text{m}/\text{min}$ ,  $\beta = 0.083 \mu\text{m}/\text{min}$ ,  $n_{\text{tot}} = 37.63 \mu\text{m}$ , and  $\ell_1^0 = \ell_2^0 = 1.74 \mu\text{m}$ .

We now will use these parameters to inform a severing experiment. We start with one filament being the steady state length from the pH shock experiment. We assume that the material that was in the severed flagellum is gone, so that the only precursor available is that which was in the non-severed flagellum and in the cytoplasm. We then numerically solve for the dynamics. The result is shown in Fig. 8. We see the main feature of shrinkage of the intact microtubule while the severed one grows is captured in this model. However, the time scale is too long. This is possibly due to that fact that the parameters were obtained from fitting the pH shock experiment, which has different conditions. We also do not capture the regrowth of the two flagella together that was observed in the experiment. This implies that the cell is making more precursor, which we may want to include in a refinement. This also raises the question of how the cell senses and controls the total amount of tubulin it produces.

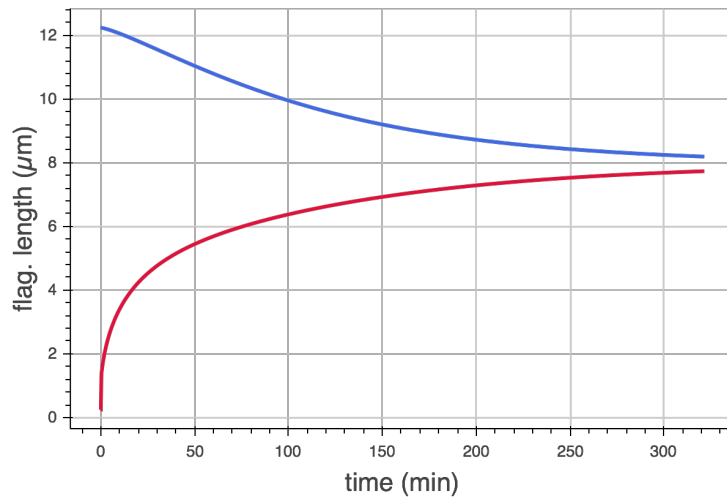


Figure 8: Numerical calculation of severing experiment. The red line shows the length of the severed flagellum and the blue the intact flagellum.

### 3.2 Conclusions from this exercise

In doing this exercise in mathematizing cartoons, we have produced models that can predict experimental results. In doing so, we have exposed gaps in our understanding. We saw both quantitative (wrong time scales) and qualitative (no co-growth) failures of our model. This process of proposing physical models and devising and performing experiments to challenge them, is what learning about physical processes in cells is all about.

## 4 Statistical mechanics and ligand-receptor binding

In the last lecture, we explored how to mathematize cartoons, mostly where the underlying physics could be described with mass action kinetics. Today, we will learn how to mathematize cartoons where the physical principles involved rest on **statistical mechanics**. We will have in mind an example, ligand receptor binding, as we do this.

### 4.1 Motivation: ligand-receptor binding

A cartoon for ligand-receptor binding is shown in Fig. 9. We are interested in computing the probability that a given receptor is bound with a ligand. We will call this  $p_{\text{bound}}$ . We model the receptor as fixed, sitting in a sea of solvent and ligand. Either one or zero ligands may be bound to the receptor at any given time.

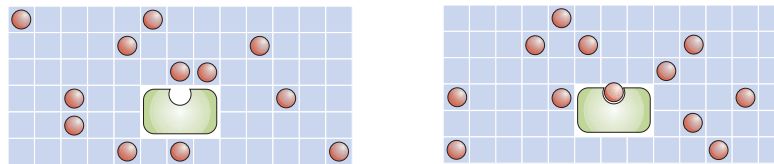


Figure 9: A schematic for ligand-receptor binding. At left, we have a single receptor (in green) and many ligands. Each square in the grid can either be occupied by a ligand or a solvent molecule. In this image, the receptor does not have a ligand bound to it. In the right image, a ligand is bound to the receptor. Figure adapted from Fig. 6.1 of *PBoC2*.

We define a “state,” or “microstate,” of this system by the configuration of the  $L$  ligands among the  $N$  available spaces on the grid. Some of these states have the receptor bound. In this case, there are  $L - 1$  receptors free to move about the available spaces out in the solvent.

The probability of the receptor being bound is

$$p_{\text{bound}} = \sum_{i \in \text{states with bound receptor}} p_i, \quad (4.1)$$

where  $p_i$  is the probability of being in state  $i$ . So, in order to compute  $p_{\text{bound}}$ , we need to compute  $p_i$  for a given state. This is where statistical mechanics comes in.

### 4.2 Derivation of the Boltzmann distribution

We will develop an expression for  $p_i$  more generally for any system with an associated set of discrete states. The states are indexed by  $i$ , and each has an energy  $E_i$  associated with it. We will take an approach along the lines of section 6.1.2 of *PBoC2*, which is a bit unconventional for statistical physics textbooks. We will maximize **informational entropy** in our treatment, following E. T. Jaynes, *Phys. Rev.*, **106**, 620–630, 1957. The abstract of that paper very cleanly and clearly captures the notion of what we are trying to do here.

Information theory provides a constructive criterion for setting up probability distributions on the basis of partial knowledge, and leads to a type of statistical inference which is called the maximum-entropy estimate. It is the least biased estimate possible on the given information; i.e., it is maximally noncommittal with regard to missing information. If one considers statistical mechanics as a form of statistical inference rather than as a physical theory, it is found that the usual computational rules, starting with the determination of the partition function, are an immediate consequence of the maximum-entropy principle. In the resulting “subjective statistical mechanics,” the usual rules are thus justified independently of any physical argument, and in particular independently of experimental verification; whether or not the results agree with experiment, they still represent the best estimates that could have been made on the basis of the information available.

It is concluded that statistical mechanics need not be regarded as a physical theory dependent for its validity on the truth of additional assumptions not contained in the laws of mechanics (such as ergodicity, metric transitivity, equal a priori probabilities, etc.). Furthermore, it is possible to maintain a sharp distinction between its physical and statistical aspects. The former consists only of the correct enumeration of the states of a system and their properties; the latter is a straightforward example of statistical inference.

Indeed, when we perform analysis using statistical mechanics in this class, we will identify the states of the system, assign their energies, and then let the machinations of statistical mechanics do the rest.

### 4.2.1 The Shannon entropy

The problem of specifying  $p_i$  is really open-ended. As Jaynes suggested, we can use maximum-entropy principles to derive an expression for  $p_i$ . The entropy he is talking about is the **Shannon entropy**, named after Claude Shannon, who published its mathematical form in 1948, also known as the **informational entropy**. I will state the definition of the entropy associated with a discrete probability distribution, and then give a short discussion on what it means intuitively.

$$S = -K \sum_i p_i \ln p_i, \quad (4.2)$$

where  $K$  is an arbitrary positive constant. It is understood that all  $p_i$ 's are nonnegative and that  $p_i \ln p_i \rightarrow 0$  as  $p_i$  tends toward zero.

We can think of entropy as a measure of ignorance, or of unbiasedness. For example, an unbiased coin will give heads in half of the flips, so the probability of getting heads is  $p_h = 1/2$ . We can choose  $K$  such that

$$S = - \sum_i p_i \log_2 p_i = -p_h \log_2 p_h - (1 - p_h) \log_2 (1 - p_h). \quad (4.3)$$

So, if  $p_h = 1/2$ ,  $S = 1$  bit, where a “bit” is the unit of entropy when we have chosen  $K$  as we have. Now, let's say  $p_h = (1 + \varepsilon)/2$ , where  $\varepsilon \in [-1, 1]$ . Now, we have

$$\begin{aligned} S &= -\frac{1+\varepsilon}{2} \log_2 \frac{1+\varepsilon}{2} - \frac{1-\varepsilon}{2} \log_2 \frac{1-\varepsilon}{2} \\ &= -\frac{1}{2} \log_2 \frac{(1+\varepsilon)(1-\varepsilon)}{4} - \frac{\varepsilon}{2} \log_2 \frac{1+\varepsilon}{1-\varepsilon} \end{aligned}$$

$$\begin{aligned}
&= 1 - \log_2(1 - \varepsilon^2) - \frac{\varepsilon}{2} \log_2 \frac{1 + \varepsilon}{1 - \varepsilon} \\
&= 1 - \log_2(1 - \varepsilon^2) - \frac{|\varepsilon|}{2} \log_2 \frac{1 + |\varepsilon|}{1 - |\varepsilon|}.
\end{aligned} \tag{4.4}$$

Looking at the three terms, we have a constant plus two monotonically decreasing functions of  $|\varepsilon|$ . Further, if  $|\varepsilon| = 1$ , we get  $S = 0$ . So, the maximal entropy is when  $\varepsilon$ , the bias of the coin, is zero. The entropy is minimal when  $|\varepsilon| = 1$ , which means that we know the outcome of the coin toss ahead of time.

Now, imagine that instead of flipping a fair coin (which has two sides), we roll a fair 8-sided die. The entropy associated with the probability distribution for the die is

$$S = - \sum_i p_i \log_2 p_i = -8 \left( \frac{1}{8} \log_2 \frac{1}{8} \right) = 3 \text{ bits.} \tag{4.5}$$

So, the entropy for a fair 8-sided die is greater than that of a fair coin. This makes sense; we are more ignorant as to the result we would expect from an 8-sided die than from a two-sided coin.

It turns out that there is only one way to define entropy that satisfies a set of *desiderata*, or desired qualities about entropy, our measure of ignorance, or unbiasedness. These desiderata are, loosely,

1. The entropy is continuous in  $p_i$ .
2. If all  $p_i$  are equal, the entropy is monotonic in  $p_i$ . (Thus, the probability distribution describing the outcomes of a roll of a fair 8-sided die should have greater entropy than that describing a fair coin flip.)
3. Arbitrary grouping of events does not change the entropy (the so-called composition law).

Shannon proved that the *only* function that has these properties is in fact the Shannon entropy, equation 4.2.

### 4.2.2 The maximal entropy distribution

To be maximally unbiased, or to use *only* the information we have about a system to infer  $p_i$ , we must choose  $p_i$  that maximizes the entropy. To do this, we differentiate the entropy with respect to  $p_i$  and set the derivative equal to zero.

$$\frac{\partial S}{\partial p_j} = -K \frac{\partial}{\partial p_j} \sum_i p_i \ln p_i = -K(1 + \ln p_j) = 0 \Rightarrow p_j = e^{-1}. \tag{4.6}$$

I put this equation in gray because this is *not* what we should do! Clearly this cannot be right, since the probability distribution is not normalized, i.e.,  $\sum_i p_i \neq 1$ .

So, we need to do a *constrained* maximization. Specifically, we need to impose the constraint that  $\sum_i p_i = 1$ , as is always the case. We impose further that  $p_i$  has a well-defined expectation value for the energy,

$$\langle E \rangle = \sum_i p_i E_i. \tag{4.7}$$

To impose the constraints in the maximization problem, we use the **method of Lagrange multipliers**, which is described on pages 254–255 in *PBoC2*. The idea is that we add zero to  $S(p_i)$ , where the

“zero” we add is defined by the constraints, with a multiplier and then minimize that function over  $p_i$  and the multipliers. We call this function the Lagrangian.

$$\begin{aligned}\mathcal{L}(p_i, \alpha, \beta) &= S + \alpha \left( 1 - \sum_i p_i \right) + \beta \left( \langle E \rangle - \sum_i p_i E_i \right) \\ &= -K \sum_i p_i \ln p_i + \alpha \left( 1 - \sum_i p_i \right) + \beta \left( \langle E \rangle - \sum_i p_i E_i \right),\end{aligned}\quad (4.8)$$

where  $\alpha$  and  $\beta$  are the Lagrange multipliers. Necessary conditions for  $p_i, \alpha$ , and  $\beta$  to be maximal are that

$$\frac{\partial \mathcal{L}}{\partial p_j} = 0 \quad \forall j,\quad (4.9)$$

$$\frac{\partial \mathcal{L}}{\partial \alpha} = 0,\quad (4.10)$$

$$\frac{\partial \mathcal{L}}{\partial \beta} = 0.\quad (4.11)$$

The last two conditions just mean that the constraints are satisfied, since they reduce to

$$1 - \sum_i p_i = 0,\quad (4.12)$$

$$\langle E \rangle - \sum_i p_i E_i = 0.\quad (4.13)$$

Now, if the constraints are affine (meaning that their second derivative with respect to  $p_i$  vanishes, which they do) and the entropy is strictly concave (its matrix of second derivatives, called the Hessian, is negative definite), then the necessary conditions are sufficient for optimality. Entry  $jk$  of the Hessian is

$$\frac{\partial^2 S}{\partial p_i \partial p_j} = -\frac{\delta_{jk}}{p_j},\quad (4.14)$$

where  $\delta_{jk}$  is the Kronecker delta ( $\delta_{jk} = 1$  for  $j = k$  and 0 otherwise). This means that the Hessian is diagonal with negative entries, so it is negative definite. Therefore, we need only to solve equations (4.9) through (4.11) to determine the maximum entropy probability distribution,  $p_i$ .

Now, we will find where the derivative of the Lagrangian with respect to  $p_j$  is zero.

$$\frac{\partial \mathcal{L}}{\partial p_j} = -K(1 + \ln p_j) - \alpha - \beta E_j = 0.\quad (4.15)$$

Solving for  $p_j$  gives

$$p_j = e^{-\alpha} e^{-\beta E_j},\quad (4.16)$$

where we have absorbed constants such that  $1 + \alpha/K \rightarrow \alpha$  and  $\beta/K \rightarrow \beta$ . Now, using the normalization constraint, we have

$$\sum_i p_i = e^{-\alpha} \sum_i e^{-\beta E_i} = 1,\quad (4.17)$$

so

$$e^\alpha = \sum_i e^{-\beta E_i} \equiv Z, \quad (4.18)$$

where we have defined the **partition function**  $Z$ . The second constraint,  $\langle E \rangle = \sum_i p_i E_i$  is automatically satisfied by definition, so we have arrived at our maximum entropy probability distribution. It is an exponential distribution.

$$p_i = \frac{e^{-\beta E_i}}{Z}. \quad (4.19)$$

### 4.2.3 Connection to thermodynamics

While we have derived an expression for  $p_i$ , we still do not know the physical meaning of the Lagrange multiplier  $\beta$ . We know only that it must have dimensions of inverse energy, since  $\beta E_i$  must be dimensionless. To connect  $\beta$  to physical quantities, we turn to thermodynamics. Thermodynamics deals with observed quantities in large systems. The internal energy is  $\langle E \rangle$ . We can write the combined first and second law of thermodynamics as

$$dS = \frac{1}{T} d\langle E \rangle. \quad (4.20)$$

Then,

$$\frac{\partial S}{\partial \langle E \rangle} = \frac{1}{T}. \quad (4.21)$$

To compute the derivative of the entropy, we first write it in a more convenient form using our derived expression for  $p_i$ .

$$\begin{aligned} S &= -K \sum_i p_i \ln p_i = -K \sum_i p_i (-\beta E_i - \ln Z) \\ &= K\beta \sum_i p_i E_i + K \ln Z \sum_i p_i = K\beta \langle E \rangle + K \ln Z. \end{aligned} \quad (4.22)$$

Thus, we have

$$\frac{\partial S}{\partial \langle E \rangle} = K\beta = \frac{1}{T}. \quad (4.23)$$

So, for the Shannon entropy to be equal to the thermodynamic entropy,  $K\beta = 1/T$ . Thus,  $\beta = 1/KT$ . When we have equivalence to the thermodynamic entropy, we call the constant  $K$  the **Boltzmann constant**, and denote it as  $k_B$  or  $k$ . The Boltzmann constant has a value of

$$k_B = 1.38 \times 10^{-23} \text{ J/K} = 4.1 \text{ pN-nm}. \quad (4.24)$$

We will also use  $\beta \equiv 1/k_B T$  in our calculations, since it turns out to be notationally convenient. Thus, we have

$$p_i = \frac{e^{-E_i/k_B T}}{\sum_i e^{-E_i/k_B T}}. \quad (4.25)$$

The quantity  $e^{-E_i/k_B T}$  represents an unnormalized probability and is referred to as a **Boltzmann weight**. Recall that the sum of Boltzmann weights is

$$Z = \sum_i e^{-E_i/k_B T}, \quad (4.26)$$

which serves as the normalization constant of the probability, is called a **partition function**.

### 4.3 Back to ligand-receptor binding

We can now return to our ligand-receptor binding problem. We know the probability of each state,  $p_i$ , and we just need to assign energies to them to compute  $p_{\text{bound}}$ . Let the energy of a single unbound ligand be  $E_u$  and the energy of a bound ligand be  $E_b$ . Then the total energy of any state where the receptor is unbound is  $LE_u$ , where, as a reminder,  $L$  is the total number of ligands. The total energy of any state where the receptor is bound is  $E_b + (L - 1)E_u$ . Then the total statistical weight of all unbound states is equal to the number of states with unbound receptor times the Boltzmann weight of an unbound state,  $e^{-\beta E_u}$ .

We can compute the number of states with unbound ligand. The number of ways select  $L$  out of  $N$  lattice sites to be occupied by ligand is given by the binomial coefficient,  $N!/(N-L)!L!$ . This is the **multiplicity** of the bound state; i.e., the number of states with the same energy.

It helps to organize everything into a **states and weights table**.

state	energy	multiplicity	statistical weight
receptor unbound	$LE_u$	$\frac{N!}{(N-L)!L!}$	$\frac{N!}{(N-L)!L!} e^{-\beta LE_u}$
receptor bound	$E_b + (L - 1)E_u$	$\frac{N!}{(N-L+1)!(L-1)!}$	$\frac{N!}{(N-L+1)!(L-1)!} e^{-\beta(E_b+(L-1)E_u)}$

For ease of notation, we will denote the appropriate binomial coefficients as  $\Omega_u$  and  $\Omega_b$ . Then, we can compute  $p_{\text{bound}}$  as

$$p_{\text{bound}} = \frac{\Omega_b e^{-\beta(E_b+(L-1)E_u)}}{\Omega_b e^{-\beta(E_b+(L-1)E_u)} + \Omega_u e^{-\beta LE_u}} = \frac{\frac{\Omega_b}{\Omega_u} e^{-\beta(E_b-E_u)}}{1 + \frac{\Omega_b}{\Omega_u} e^{-\beta(E_b-E_u)}}. \quad (4.27)$$

Now,

$$\frac{\Omega_b}{\Omega_u} = \frac{N!}{(N-L+1)!(L-1)!} \frac{(N-L)!L!}{N!} = \frac{L}{N-L+1}. \quad (4.28)$$

Because  $L \ll N$  in a dilute solution,

$$N - L + 1 \approx N \approx N + L. \quad (4.29)$$

Using these approximate expressions allow us to write  $\Omega_b/\Omega_u$  as the **mole fraction** of ligand,  $x_L$ .

$$\frac{\Omega_b}{\Omega_u} \approx \frac{L}{N} \approx \frac{L}{N+L} = x_L. \quad (4.30)$$

So,

$$p_i = \frac{x_L e^{-\beta(E_b-E_u)}}{1 + x_L e^{-\beta(E_b-E_u)}}. \quad (4.31)$$

We can convert mole fraction to concentration by multiplying by the density of solvent, water in most physiological cases;

$$c_L = \rho_{\text{H}_2\text{O}} x_L. \quad (4.32)$$

Now, if we multiply top and bottom of our expression for  $p_i$  by unity, represented as  $\rho_{\text{H}_2\text{O}} / \rho_{\text{H}_2\text{O}}$ , we get

$$p_i = \frac{c_L e^{-\beta(E_b - E_u)} / \rho_{\text{H}_2\text{O}}}{1 + c_L e^{-\beta(E_b - E_u)} / \rho_{\text{H}_2\text{O}}}. \quad (4.33)$$

Finally, we define the **dissociation** constant  $K_d = \rho_{\text{H}_2\text{O}} e^{-\beta(E_u - E_b)}$ . We arrive at

$$p_{\text{bound}} = \frac{c_L / K_d}{1 + c_L / K_d}. \quad (4.34)$$

This is a common result (called a Langmuir isotherm) that could be seen from what you remember from general chemistry. We can take the probability of a receptor being bound as

$$p_{\text{bound}} = \frac{c_{LR}}{c_{LR} + c_R}. \quad (4.35)$$

We use the definition of the dissociation constant,

$$K_d = \frac{c_L c_R}{c_{LR}}, \quad (4.36)$$

to get

$$p_{\text{bound}} = \frac{c_L c_R / K_d}{c_L c_R / K_d + c_R} = \frac{c_L / K_d}{1 + c_L / K_d}. \quad (4.37)$$

In deriving this result, we have a clear picture about the physical origin of the dissociation constant. We also have a framework to study cases where we have more complicated states and weights.

## 4.4 Maximum entropy distributions for other ensembles

We will now use the method of maximum entropy to derive probability distributions when we know other facts about the states.

### 4.4.1 Given energy and number of particles

Now let's say that we have a system that consists of particles. Each state of the system has a well defined energy,  $E_i$  and number of particles,  $N_i$ . We should therefore have an expectation value for  $N_i$ . Now, we have three constraints for  $p_i$ .

$$\sum_i p_i = 1, \quad (4.38)$$

$$\langle E \rangle = \sum_i p_i E_i, \quad (4.39)$$

$$\langle N \rangle = \sum_i p_i N_i. \quad (4.40)$$

We construct our Lagrangian as before, but with a third Lagrange multiplier.

$$\begin{aligned} \mathcal{L} = & -k_B \sum_i p_i \ln p_i + \alpha \left( 1 - \sum_i p_i \right) + \beta \left( \langle E \rangle - \sum_i p_i E_i \right) \\ & + \gamma \left( \langle N \rangle - \sum_i p_i N_i \right). \end{aligned} \quad (4.41)$$

We take the same approach as before.

$$\frac{\partial \mathcal{L}}{\partial p_j} = -k_B(1 + \ln p_j) - \alpha - \beta E_j - \gamma N_j = 0. \quad (4.42)$$

Solving gives

$$p_j = e^{-\alpha} e^{-\beta E_j - \gamma N_j}, \quad (4.43)$$

where we have again absorbed constants:  $-1 - \alpha/k_B \rightarrow \alpha$ ,  $\beta/k_B \rightarrow \beta$ , and  $\gamma/k_B \rightarrow \gamma$ . We use the normalization condition that  $\sum_i p_i = 1$  to get

$$e^\alpha = \sum_i e^{-\beta E_j - \gamma N_j} \equiv Z. \quad (4.44)$$

To find the values of the other Lagrange multipliers that connect the entropy to the thermodynamic entropy, we do the same procedure. We first write the combined first and second law of thermodynamics.

$$dS = \frac{1}{T} d\langle E \rangle - \frac{\mu}{T} d\langle N \rangle, \quad (4.45)$$

where  $\mu$  is the chemical potential of the particles. Thus,

$$\left( \frac{\partial S}{\partial \langle N \rangle} \right)_{\langle E \rangle} = -\frac{\mu}{T}. \quad (4.46)$$

Going back to the expression we wrote for the probability  $p_i$  and the partition function,

$$\begin{aligned} S = & -k_B \sum_i p_i \ln p_i = -k_B \sum_i p_i (-\beta E_i - \gamma N_i - \ln Z) \\ = & k_B \ln Z + k_B \beta \langle E_i \rangle + k_B \gamma \langle N \rangle. \end{aligned} \quad (4.47)$$

So,

$$\left( \frac{\partial S}{\partial \langle N \rangle} \right)_{\langle E \rangle} = k_B \gamma = -\frac{\mu}{T}. \quad (4.48)$$

Thus, we have  $\gamma = -\mu/k_B T$ . We again get  $\beta = 1/k_B T$  in a similar manner. Thus, we have

$$p_i = \frac{e^{-\beta(E_i - \mu N_i)}}{\sum_i e^{-\beta(E_i - \mu N_i)}}. \quad (4.49)$$

#### 4.4.2 A general thermodynamic conjugate pair

We see a pattern here. Let's say that a given state has associated with it an energy  $E_i$ , and another arbitrary extensive property  $X_i$  with a well-defined expectation value  $\langle X \rangle$ . Then, the maximum entropy distribution is

$$p_i = \frac{e^{-\beta E_i - \lambda X_i}}{\mathcal{Z}}, \quad (4.50)$$

where

$$\mathcal{Z} = \sum_i e^{-\beta E_i - \lambda X_i}, \quad (4.51)$$

with  $\lambda$  being a Lagrange multiplier. To link  $\lambda$  to a physical quantity, it always ends up being the thermodynamic conjugate variable to  $\langle X \rangle$  divided by  $kT$ . We can have many such extensive properties. So, if we index these properties by  $k$ , we have, generally,

$$p_i = \frac{1}{\mathcal{Z}} \exp \left\{ -\frac{1}{k_B T} \left( E_i + \sum_k y_k X_k \right) \right\}, \quad (4.52)$$

where  $y_k$  denotes the thermodynamic conjugate variable to  $X_k$  and

$$\mathcal{Z} = \sum_i \exp \left\{ -\frac{1}{k_B T} \left( E_i + \sum_k y_k X_k \right) \right\}. \quad (4.53)$$

#### 4.5 Another look at ligand-receptor binding

Let's take another look at ligand-receptor binding using our new tools. We'll reframe how we look at the system. We focus on the receptor, knowing there is a pool of ligands immediately around it. In the *immediate* vicinity of the receptor, there can only be zero or one ligand. In the latter case, the ligand is bound. So, the number of ligands in the system can fluctuate, so we can define each state to have an energy  $E_i$  and a number of ligands,  $L_i$ . If  $\mu$  is the chemical potential of a ligand, then we have a new states and weights table.

state	energy	multiplicity	statistical weight
receptor unbound	$E_u$	1	$e^{-\beta E_u}$
receptor bound	$E_b$	1	$e^{-\beta(E_b - \mu)}$

We can then readily compute  $p_{\text{bound}}$ .

$$p_{\text{bound}} = \frac{e^{-\beta(E_b - \mu)}}{e^{-\beta(E_b - \mu)} + e^{-\beta E_u}} = \frac{e^{-\beta(E_b - E_u - \mu)}}{1 + e^{-\beta(E_b - E_u - \mu)}}. \quad (4.54)$$

Now, as derived in section 6.2.2 of *PBoC2* (we will not derive it here), for a dilute solution, the chemical potential of solute species  $k$  is

$$\mu_k = \mu_k^0 + k_B T \ln x_k. \quad (4.55)$$

The chemical potential for the solvent is

$$\mu_{\text{solv}} = \mu_{\text{solv}}^0 - k_B T \sum_k x_k. \quad (4.56)$$

If we insert the chemical potential for solute into our expression for  $p_{\text{bound}}$ , we get

$$p_{\text{bound}} = \frac{x_L e^{-\beta(E_b - E_u - \mu^0)}}{1 + x_L e^{-\beta(E_b - E_u - \mu^0)}} = \frac{c_L / K_d}{1 + c_L / K_d} = \frac{c_L}{K_d + c_L}, \quad (4.57)$$

the same expression as before with

$$K_d = e^{-\beta(E_u + \mu^0 - E_b)}. \quad (4.58)$$

Note that there is a difference in the definition of  $K_d$ , which is due to the subtle difference in the definition of the energies of the states. In our previous treatment, we defined  $E_u$  to be the energy of a ligand when unbound. We tacitly assumed that the energy of the receptor when unbound was zero. Here,  $E_u$  is the energy of the receptor when unbound and  $\mu^0$  is the energy of a single ligand alone in solution.

## 5 Two-state models case study: mechanosensitive ion channels

In the last lecture, we worked through some basic ideas of statistical mechanics and applied them to ligand-receptor binding. The simple ligand-receptor binding example belongs to a class of **two-state models**. As the name suggests, these are models where there are two states to consider. In the ligand-receptor binding example, there were two states for the receptor, bound and unbound. A great many systems may be modeled with two-state models, and we can use the tools of statistical mechanics to derive useful expressions describing their equilibrium behavior.

In this lecture, we will investigate another two-state model, this time ion channels. **Ion channels** are transmembrane protein complexes that can open and close to mediate the transport of ions in and out of a cell. We will use mechanosensitive ion channels, such as Mscl in *E. coli* as our first case study in two-state models.

### 5.1 Experimental analysis of ion channels

Bert Sakmann and Erwin Neher developed the **patch clamp technique** whereby researchers can measure current through a single ion channel. Such readings can give traces like those shown in Fig. 10.

If we consider a long time trace, we can compute  $p_{\text{open}}$ , the equilibrium probability that an ion channel is open, as the total time during the trace where the channel is open divided by the total time of the trace. The greater  $p_{\text{open}}$  is, the more ions can flow through it per unit time.

### 5.2 A simple two-state model for an ion channel

In order to compute  $p_{\text{open}}$  for an ion channel, we define two states, open and closed. We can assign energies to these two states,  $E_{\text{open}}$  and  $E_{\text{closed}}$ . We can then write a states and weights table, as in the previous lecture.

state	energy	statistical weight
closed	$E_{\text{closed}}$	$e^{-\beta E_{\text{closed}}}$
open	$E_{\text{open}}$	$e^{-\beta E_{\text{open}}}$

We can then compute the probability that the channel is open as

$$p_{\text{open}} = \frac{e^{-\beta E_{\text{open}}}}{e^{-\beta E_{\text{open}}} + e^{-\beta E_{\text{closed}}}} = \frac{e^{-\beta(E_{\text{open}} - E_{\text{closed}})}}{1 + e^{-\beta(E_{\text{open}} - E_{\text{closed}})}}. \quad (5.1)$$

Naturally, the open and closed energies will depend on the voltage, which will give  $p_{\text{open}}$  as a function of voltage. This is an example of a **voltage gaged ion channel**. But for our present case study, we will consider **mechanosensitive ion channels**, where  $p_{\text{open}}$  (via the energy of the two states of the channel) depends on the *tension* in the membrane. So, our goal is to write

$$E_{\text{open}} = E_{\text{open}}(\gamma), \quad (5.2)$$

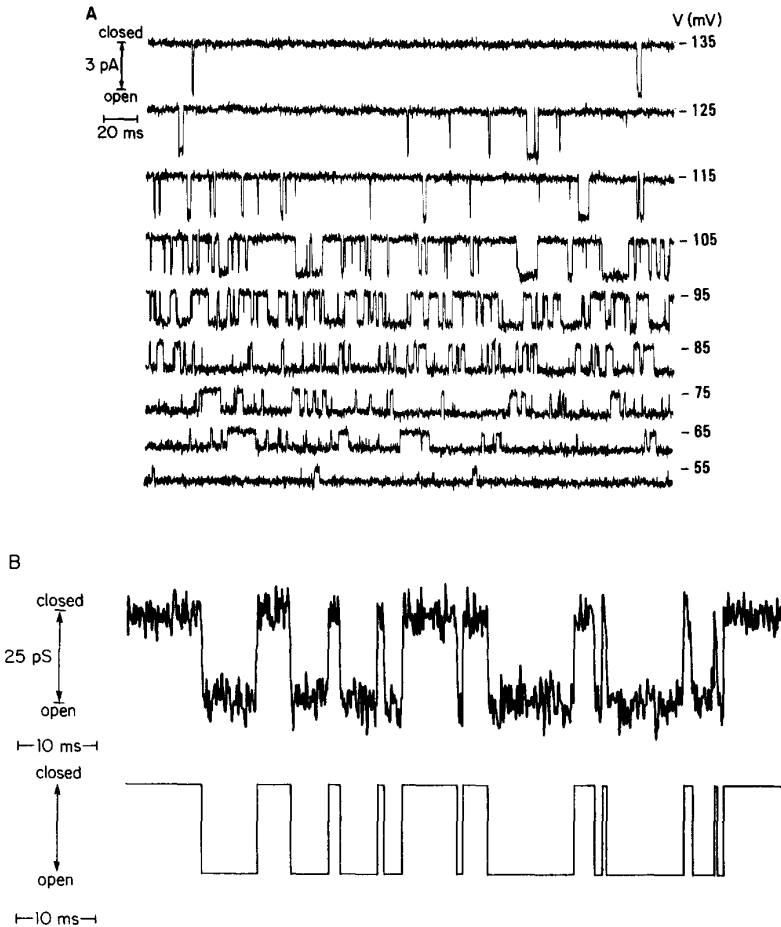


Figure 10: Patch clamp recordings of a single sodium ion channel in a reconstituted lipid bilayer. A. Recordings of current taken at different voltages. For a voltage of high magnitude, the channel has a constant current, indicating it is almost always open. For voltage of low magnitude, it is closed. B. Detail of the trace at -95 mV. The bottom trace shows a digitized version, displaying when the channel is open or closed. Figure taken from [Keller, et al., J. Gen. Physiol., 88, 1-13, 1986.](#)

where  $\gamma$  is the membrane tension, and then compute  $p_{\text{open}}$  using the Boltzmann weights.

Before we proceed to this calculation, we first provide some context as to why a cell would need mechanosensitive ion channels to deal with sudden changes in pressure due to osmotic shock.

### 5.3 Osmotic pressure

**Osmotic pressure**, is a pressure exerted across a membrane due to differences in concentration of solute on either side of the membrane. In the case of Mscl, the solute is positive ions. We can understand osmotic pressure by looking at the thermodynamics of dilute solutions. The chemical potential of water on either side of a cell membrane, must be equal at equilibrium. That is, the chemical poten-

tial of water in the cell must equal that in the environment.

$$\mu_{\text{H}_2\text{O}}^{\text{cell}} = \mu_{\text{H}_2\text{O}}^{\text{env}}. \quad (5.3)$$

In the previous lecture in equation (4.56), I stated without proof (see section 6.2.2 of *PBoC2*) that the chemical potential of water in a dilute solution is

$$\mu_{\text{H}_2\text{O}}(p, T) = \mu_{\text{H}_2\text{O}}^0(p, T) - k_B T x, \quad (5.4)$$

where  $x$  is the mole fraction of solute molecules. Note that the chemical potential is in general a function of pressure and temperature. So, at equilibrium, we have

$$\mu_{\text{H}_2\text{O}}^0(p_{\text{cell}}, T) - k_B T x_{\text{cell}} = \mu_{\text{H}_2\text{O}}^0(p_{\text{env}}, T) - k_B T x_{\text{env}}. \quad (5.5)$$

This implies that

$$\mu_{\text{H}_2\text{O}}^0(p_{\text{cell}}, T) - \mu_{\text{H}_2\text{O}}^0(p_{\text{env}}, T) = k_B T(x_{\text{cell}} - x_{\text{env}}). \quad (5.6)$$

Note that we have assumed thermal equilibrium. Then, if the concentration of solute molecules in the cell is different than in the environment,  $x_{\text{cell}} \neq x_{\text{env}}$ , then the inside and outside of the cell must have different pressure. This difference in pressure,  $\Pi \equiv p_{\text{cell}} - p_{\text{env}}$ , is called the osmotic pressure. To proceed, we can expand the left hand side of the above equation about  $\Pi = p_{\text{cell}} - p_{\text{env}} = 0$  to first order to get

$$\mu_{\text{H}_2\text{O}}^0(p_{\text{cell}}, T) - \mu_{\text{H}_2\text{O}}^0(p_{\text{env}}, T) \approx \left( \frac{\partial \mu_{\text{H}_2\text{O}}^0}{\partial p} \right) \Pi. \quad (5.7)$$

The differential in this equation is the volume of a water molecule, as we know from thermodynamics.<sup>3</sup>

$$\frac{\partial \mu_{\text{H}_2\text{O}}^0}{\partial p} = v_{\text{H}_2\text{O}} = V/N_{\text{H}_2\text{O}}. \quad (5.8)$$

Thus, we have

$$V/N_{\text{H}_2\text{O}} \Pi = k_B T(x_{\text{cell}} - x_{\text{env}}). \quad (5.9)$$

Recall that  $x_{\text{cell}} \approx N_{\text{solute}}^{\text{cell}}/N_{\text{H}_2\text{O}}$ . Using this fact, we have

$$\Pi = k_B T(c_{\text{cell}} - c_{\text{env}}), \quad (5.10)$$

where  $c$  represents a concentration,  $N_{\text{solute}}/V$ .

The typical concentration of positive ions in *E. coli* is approximately 200 mM ([BNID 104049](#)), or about 0.1 molecules per cubic nanometer. Thus, the osmotic pressure in an *E. coli* cell, assuming that  $c_{\text{env}} \approx 0$  (which would be the case if you put a cell in deionized water) is

$$\Pi \approx 4 \text{ pN}\cdot\text{nm} \times 0.1 \text{ nm}^{-3} = 0.4 \text{ pN}/\text{nm}^2. \quad (5.11)$$

Given the conversion that  $1 \text{ pN}/\text{nm}^2 \approx 10 \text{ atm}$ , the osmotic pressure in *E. coli* in deionized water is approximately 4 atm. The cell can handle the pressure with its cell wall, but you can imagine that if you rapidly changed the ionic conditions outside the cell, it suddenly has to withstand a very large pressure, which can lead to the cell bursting. Mechanosensitive ion channels respond to increased membrane tension as a result of osmotic shock to let ions in or out to relieve osmotic pressure.

---

<sup>3</sup>To see this, consider the total Legendre transform of the free energy,  $0 = -S dT + V dp - N d\mu$ , and compute  $(\partial \mu / \partial p)_T$ .

## 5.4 Tension and the ion channel

When the ion channel is closed, the membrane is more stretched than when it is open. This is because a closed channel pulls the membrane more taught, and an open membrane can relieve the tension. The opening of the channel leads to a change in total area of the surface of the cell,  $\Delta A$ . We should take into account the areal stretch of the membrane when considering the energetics of channel opening. So, we have  $E^{\text{stretch}} = E_{\text{stretch}}(\Delta A)$ , and define  $\Delta A = 0$  for the closed state. We write  $E^{\text{stretch}}$  as a Taylor series in  $\Delta A$  about  $\Delta A = 0$ . To first order,

$$E_{\text{open}}^{\text{stretch}} = E_{\text{closed}}^{\text{stretch}} - \gamma \Delta A. \quad (5.12)$$

It is clear from the Taylor expansion that  $\gamma$  is a tension (with dimension force per length). We have chosen a negative sign to ensure that  $\gamma$  is positive under our definition that  $\Delta A$  is positive. The stretching energy of the open state is less than the closed state. Thus, we have

$$E_{\text{closed}} = E_{\text{closed}}^0 + E_{\text{closed}}^{\text{stretch}}, \quad (5.13)$$

$$E_{\text{open}} = E_{\text{open}}^0 + E_{\text{closed}}^{\text{stretch}} - \gamma \Delta A. \quad (5.14)$$

We have divided the energy of a state into the energetics associated with the state of the channel itself, marked by a naught superscript, and the energy associated with stretching the membrane. If we define  $E_{\text{closed}}^0 + E_{\text{closed}}^{\text{stretch}}$  as our reference energy, and  $\epsilon \equiv E_{\text{open}}^0 - E_{\text{closed}}^0$ , our updated states and weights table is as follows.

state	energy	statistical weight
closed	0	1
open	$\epsilon - \gamma \Delta A$	$e^{-\beta(\epsilon - \gamma \Delta A)}$

We can now write our updated expression for the probability of the ion channel being open as a function of the membrane tension  $\gamma$ .

$$p_{\text{open}} = \frac{e^{-\beta(\epsilon - \gamma \Delta A)}}{1 + e^{-\beta(\epsilon - \gamma \Delta A)}}. \quad (5.15)$$

## 5.5 Determining the parameters

As we have seen again and again in the course, physical modeling of cellular systems exposes measurable parameters and testable hypotheses. So, can we do a patch clamp experiment to determine the parameters? Perozo and coworkers ([Perozo, et al., Nat. Struct. Biol., 9, 696–703, 2002](#)) did just that. They adjusted the applied pressure across a reconstituted membrane and could measure the current through a single Mscl channel. They then computed  $p_{\text{open}}$  as I described above for the voltage gated ion channel. I digitized the data from their measurements and show them in Fig. 11.

As we will derive when we do membrane mechanics later in the course, the tension  $\gamma$  in the membrane is directly proportional to the applied pressure. Defining the constant of proportionality to be  $\alpha$ , we can write the theoretical curve describing the experimental data as

$$p_{\text{open}} = \frac{e^{-\beta(\epsilon - \alpha p \Delta A)}}{1 + e^{-\beta(\epsilon - \alpha p \Delta A)}}, \quad (5.16)$$

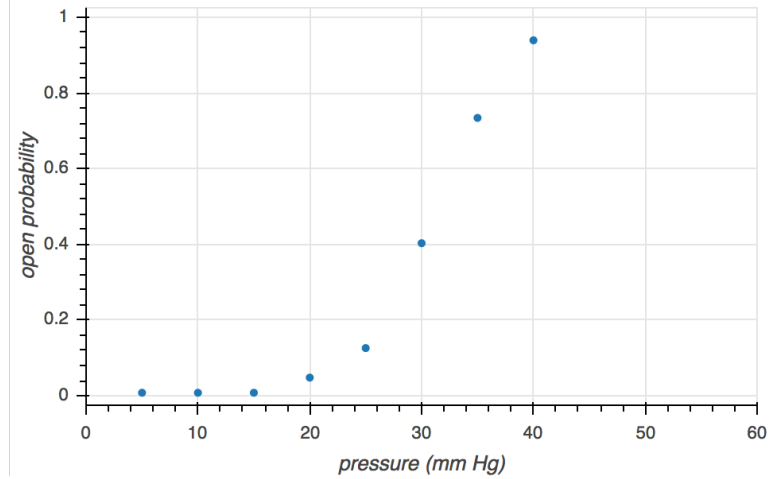


Figure 11: Digitized data from a patch clamp experiment from Perozo, et al., *Nat. Struct. Biol.*, 9, 696–703, 2002.

where  $p$  is the applied pressure. This expression has five parameters,  $\beta$ ,  $\alpha$ ,  $\Delta A$ ,  $E_{\text{open}}^0$ , and  $E_{\text{closed}}^0$ , where the last two are present in  $\varepsilon$ . As we can already see, the equation we have derived for  $p_{\text{open}}$  can only delineate the *difference* in the open and closed energies of the ion channel, parametrized by  $\varepsilon$ . The experiments were done at room temperature (about 295 K), so we know  $\beta \approx 1/(4 \text{ pN-nm})$ . We might know what  $\Delta A$  is from structural studies, but let's assume we do not know it. By defining  $a = \alpha \Delta A$ , and re-writing  $p_{\text{open}}$ ,

$$p_{\text{open}} = \frac{e^{-\beta \varepsilon} e^{\beta a p}}{1 + e^{-\beta \varepsilon} e^{\beta a p}}, \quad (5.17)$$

we see that we can only determine two constants from measurements of  $p_{\text{open}}$  (given that we know  $\beta$ ),  $\varepsilon$ , the difference in energy of the open and closed states of the channel in the absence of tension, and  $a$ , which describes how tension on the membrane serves to open channels.

We can perform a nonlinear regression to obtain estimates for the parameters  $\beta \varepsilon$  and  $\beta a$ .<sup>4</sup> The code to do the regression appears below (with some L<sup>A</sup>T<sub>E</sub>X-based problems with displaying unicode at the very end of the script). To do the regression, we use least squares, as implement in SciPy. Performing the regression, we get that the most probable parameter values are  $\beta \varepsilon = 9.2$  and  $\beta a = 0.3 \text{ (mm Hg)}^{-1}$ . The result is shown in Fig. 12.

Interestingly, we were able to obtain that absence tension on the membrane, the energy difference between the open and closed state is about  $9 k_B T$ . This gives an open probability in the absence of tension of about  $10^{-4}$ , which would be difficult to observe experimentally by just measuring current through an un-tensed channel. This also means that in the absence of tension, the channel is almost always closed. It takes tension to open it, hence the name mechanosensitive.

This exercise has shown the power of two-state models in helping to set up experiments to probe the physical nature of ion channels.

---

<sup>4</sup>I make the usual statements about the perils of directly doing a maximum likelihood estimate for the parameters.

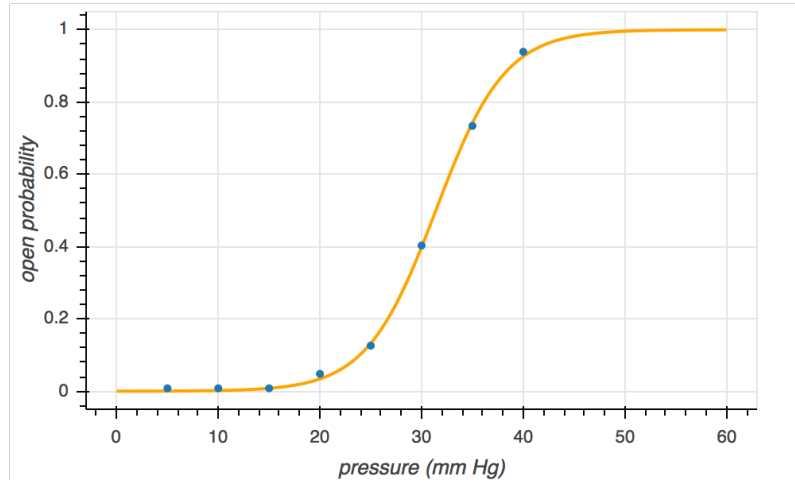


Figure 12: Curve fit of the Perozo, et al., patch clamp data.

```

1 import numpy as np
2 import scipy.optimize
3 import bokeh.plotting
4
5 # The data sets
6 pressure = np.array([5, 10, 15, 20, 25, 30, 35, 40])
7 p_open = np.array([0.008, 0.008, 0.008, 0.048,
8                   0.126 ,0.403 ,0.734 ,0.939])
9
10 # Define theoretical p_open
11 def p_open_theor(pressure, beta_epsilon, beta_a):
12     """Theoretical p_open"""
13     return 1 / (1 + np.exp(beta_epsilon - beta_a * pressure))
14
15 # Define residuals
16 def resid(params, pressure, p_open):
17     # Unpack parameters
18     beta_epsilon, beta_a = params
19
20     # Compute residuals
21     return p_open - p_open_theor(pressure, beta_epsilon, beta_a)
22
23 # Bound on parameters, first lower bounds, then upper
24 bounds = ((-np.inf, 0), (np.inf, np.inf))
25
26 # Initial guess
27 p0 = np.array([0.1, 0.1])
28
29 # Perform least squares
30 res = scipy.optimize.least_squares(resid,
31                                     p0,
32                                     args=(pressure, p_open),

```

```

33                                         bounds=bounds)

34
35 # Put out the optimal parameters
36 beta_epsilon, beta_a = res.x

37
38 # Generate smooth curve
39 pressure_smooth = np.linspace(0, 70, 200)
40 p_open_fit = p_open_theor(pressure_smooth, beta_epsilon, beta_a)

41
42 # Make the plot
43 p = bokeh.plotting.figure(plot_width=500,
44                           plot_height=300,
45                           x_axis_label='pressure (mm Hg)',
46                           y_axis_label='open probability')
47 p.line(pressure_smooth, p_open_fit, line_width=2, color='orange')
48 p.circle(pressure, p_open)
49 bokeh.io.show(p)

50
51 # Report results
52 print("""Most probable fit parameters: \beta \epsilon
53 : {0:.2f} \beta
54 a: {1:.2f} (mm Hg)""".format(beta_epsilon, beta_a))

```

perozo\_regression.py

# 6 Allostery and the Monod-Wyman-Changeux model

In a previous lecture, we used the theory of equilibrium statistical mechanics to study ligand receptor binding. We then applied a similar theoretical approach to treat a mechano-sensitive ion channel behavior. In this lecture, we extend that ligand-receptor binding theory to include more states beyond “bound” and “unbound.” As we work through the theory, we will discover some of the basic ideas behind allostery and introduce the famous Monod-Wyman-Changeux (MWC) model.

## 6.1 Allostery

Consider an enzyme that has two binding sites. One site is involved in its activity, say with binding its target substrate. We will call this the active site. The other binding site binds some other ligand. Important, when this other site is bound, the activity of the active site is either positively or negatively affected. This phenomenon, where binding of one site of a protein or protein complex affects the activity of another is called **allostery**.

We can explore allostery using the same states-and-weights approach as with the vanilla ligand-receptor binding we have already studied. In that case, we had two states, bound and unbound. Now, we also specify whether or not the receptor is active or inactive. So, there are now four states, unbound and inactive, unbound and active, bound and inactive, and bound and active. Each of these four states has an energy associated with it.

It is more convenient to treat our system to be only the receptor and possibly the single ligand bound to it. In this case, the energy of the bound state is supplemented with the chemical potential associated with taking the ligand out of solution, as we showed in lecture 4. That is, we subtract  $\mu = \mu_0 + k_B T \ln x$ , where  $x$  is the mole fraction of ligand, from the energy to get the statistical weight. This is shown in the states and weights table below.

state	description	energy	statistical weight
	unbound, inactive	$E_{ui}$	$e^{-\beta E_{ui}}$
	unbound, active	$E_{ua}$	$e^{-\beta E_{ua}}$
	bound, inactive	$E_{bi}$	$xe^{-\beta(E_{bi} - \mu_0)}$
	bound, active	$E_{ba}$	$xe^{-\beta(E_{ba} - \mu_0)}$

We are most interested in the probability that the receptor is active, which we can compute from the states and weights table.

$$\begin{aligned}
 p_{\text{active}} &= \frac{\text{sum of weights of active states}}{\text{sum of all weights}} \\
 &= \frac{e^{-\beta E_{ua}} + xe^{-\beta(E_{ba} - \mu_0)}}{e^{-\beta E_{ui}} + e^{-\beta E_{ua}} + xe^{-\beta(E_{bi} - \mu_0)} + xe^{-\beta(E_{ba} - \mu_0)}}. \tag{6.1}
 \end{aligned}$$

This can be simplified by defining dissociation constants for ligand-receptor binding when the receptor is respectively in the inactive and active states,

$$K_{di} = \rho_{H_2O} e^{-\beta(E_{ui} + \mu_0 - E_{bi})}, \quad (6.2)$$

$$K_{da} = \rho_{H_2O} e^{-\beta(E_{ua} + \mu_0 - E_{ba})}, \quad (6.3)$$

where  $\rho_{H_2O}$  is the number density of solvent. We can also use it to define the concentration of ligand as  $c = \rho_{H_2O}x$ . Then, the expression for the probability that the receptor is active is

$$\begin{aligned} p_{\text{active}} &= \frac{1 + c/K_{da}}{1 + c/K_{da} + e^{-\beta \Delta E_u} \left(1 + \frac{K_{da}}{K_{di}}(c/K_{da})\right)} \\ &= \frac{1 + c/K_{da}}{1 + c/K_{da} + e^{-\beta \Delta E_u} + e^{-\beta \Delta E_b}(c/K_{da})}, \end{aligned} \quad (6.4)$$

where  $\Delta E_u = E_{ui} - E_{ua}$  is the difference in energies of the inactive and active states in the absence of ligand and  $\Delta E_b = E_{bi} - E_{ba}$  is the difference in energies of the inactive and active states when the receptor is bound to ligand.

To understand this expression, we can consider the small and large  $c$  limits. In the small ligand concentration limit, we have

$$\text{small } c : p_{\text{active}} = \frac{1}{1 + e^{-\beta \Delta E_u}}, \quad (6.5)$$

which is what we expect from a two-state model for receptor activity that does not include binding. We will consider this to be the base case of activity, that is the probability that the receptor is active in absence of ligand. In the limit of large ligand concentration, we have

$$\text{large } c : p_{\text{active}} = \frac{1}{1 + \frac{K_{da}}{K_{di}} e^{-\beta \Delta E_u}} = \frac{1}{1 + e^{-\beta \Delta E_b}}. \quad (6.6)$$

So, if the ratio of the dissociation constants,  $K_{da}/K_{di}$ , is less than one, i.e., if the ligand binds more tightly to the active state than to the inactive state, the activity of the receptor is enhanced by the ligand. This is allosteric; binding of a ligand at one site of an enzyme enhances activity at another.

To better visualize the how  $p_{\text{active}}$  varies with ligand concentration, see Fig. 13 for a plot.

It is also useful to quantify how effective allosteric activation can be compared to the base case of no ligands. The maximum fold change in activity compared to the base case is found by dividing the large  $c$  limit of  $p_{\text{active}}$  by the base case  $p_{\text{active}}$ .

$$\text{max fold change} = \frac{\text{large } c \text{ limit of } p_{\text{active}}}{\text{small } c \text{ limit of } p_{\text{active}}} = \frac{1 + e^{-\beta \Delta E_u}}{1 + \frac{K_{da}}{K_{di}} e^{-\beta \Delta E_u}} = \frac{1 + e^{-\beta \Delta E_u}}{1 + e^{-\beta \Delta E_b}}. \quad (6.7)$$

So, the maximum achievable fold change is set by  $1 + e^{-\beta \Delta E_u}$ . The larger the energy difference between the active and inactive unbound states, the more effective the ligand-mediated allosteric activation.

**The Monod-Wyman-Changeux model.** The example we just worked out is an example of a Monod-Wyman-Changeux (MWC) model. The main idea behind the MWC model is the presence of two states, whether or not ligand is bound, and that ligand can bind in either configuration. As we have seen, ligand binding shifts the equilibrium between the two states. It is a simple and beautiful idea, and we will come to see that it is very powerful and ubiquitous throughout cell biology.

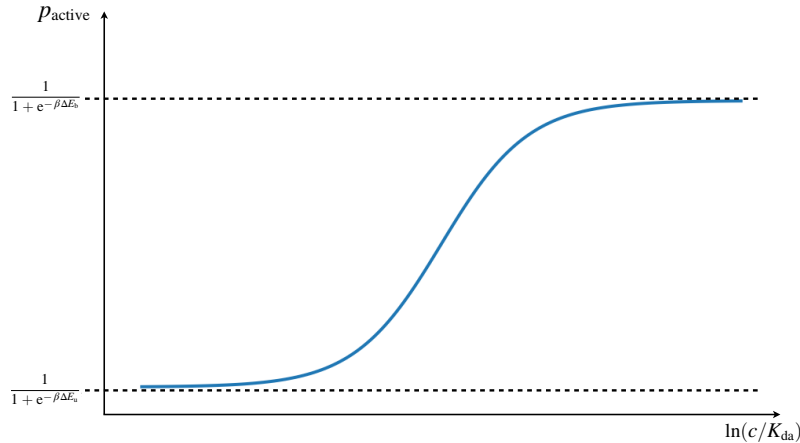


Figure 13: A sketch of the probability that the receptor is active as a function of ligand concentration.

## 6.2 Ligand-gated ion channels

In the last lecture, we considered the statistical mechanics of a mechano-sensitive ion channel. We will not turn to ion channels that are **ligand-gated**, and treat them using the MWC framework. That is, the ion channel has two states, open and closed, and the energetics of ligand binding in those two states varies.

In our model, we will assume that there are two binding sites for ligands on the channel. We may therefore have four binding states, no sites bound, site one bound, site two bound, and both sites bound. With the two states of the ion channel, open and closed, that leaves eight total states to enumerate. We will assume that both binding sites have the same energy, such that the single bound open states have the same energy, as do the singly bound closed states. We again use the convenient method of including the chemical potential of the ligand in the statistical weights so we do not need to explicitly count spatial configurational states of the ligand. With these considerations in mind, we can write the states-and-weights table.

state	energy	statistical weight
	$2E_{uc}$	$e^{-2\beta E_{uc}}$
	$E_{uc} + E_{bc}$	$x e^{-\beta(E_{uc} + E_{bc} - \mu_0)}$
	$E_{uc} + E_{bc}$	$x e^{-\beta(E_{uc} + E_{bc} - \mu_0)}$
	$2E_{bc}$	$x^2 e^{-2\beta(E_{bc} - \mu_0)}$
	$2E_{uo}$	$e^{-2\beta E_{uo}}$
	$E_{uo} + E_{bo}$	$x e^{-\beta(E_{uo} + E_{bo} - \mu_0)}$
	$E_{uo} + E_{bo}$	$x e^{-\beta(E_{uo} + E_{bo} - \mu_0)}$
	$2E_{bo}$	$x^2 e^{-2\beta(E_{bo} - \mu_0)}$

For the case of this ion channel, the “active state” is the open state. So, we wish to compute  $p_{open}$ . We directly read off the states and weights table to compute it.

$$\begin{aligned}
p_{open} &= \frac{\text{sum of weights of open states}}{\text{sum of all weights}} \\
&= \frac{e^{-2\beta E_{uo}} + 2x e^{-\beta(E_{uo} + E_{bo} - \mu_0)} + x^2 e^{-2\beta(E_{bo} - \mu_0)}}{e^{-2\beta E_{uc}} + 2x e^{-\beta(E_{uc} + E_{bc} - \mu_0)} + x^2 e^{-2\beta(E_{bc} - \mu_0)} + e^{-2\beta E_{uo}} + 2x e^{-\beta(E_{uo} + E_{bo} - \mu_0)} + x^2 e^{-2\beta(E_{bo} - \mu_0)}} \\
&= \frac{1 + 2x e^{-\beta(E_{bo} - E_{uo} - \mu_0)} + x^2 e^{-2\beta(E_{bo} - E_{uo} - \mu_0)}}{1 + 2x e^{-\beta(E_{bo} - E_{uo} - \mu_0)} + x^2 e^{-2\beta(E_{bo} - E_{uo} - \mu_0)} + e^{-\beta \Delta E_u} (1 + 2x e^{-\beta(E_{bc} - E_{uc} - \mu_0)} + x^2 e^{-2\beta(E_{bc} - E_{uc} - \mu_0)})} \\
&= \frac{(1 + c/K_{do})^2}{(1 + c/K_{do})^2 + e^{-2\beta \Delta E_u} \left(1 + \frac{K_{do}}{K_{dc}} (c/K_{do})\right)^2} \\
&= \frac{(1 + c/K_{do})^2}{(1 + c/K_{do})^2 + (e^{-\beta \Delta E_u} + e^{-\beta \Delta E_b} (c/K_{do}))^2}
\end{aligned} \tag{6.8}$$

where

$$\Delta E_u = E_{uc} - E_{uo}, \tag{6.9}$$

$$\Delta E_b = E_{bc} - E_{bo}, \tag{6.10}$$

$$K_{do} = \rho_{H_2O} e^{-\beta(E_{uo} + \mu_0 - E_{bo})}, \tag{6.11}$$

$$K_{dc} = \rho_{H_2C} e^{-\beta(E_{uc} + \mu_0 - E_{bc})}. \tag{6.12}$$

The functional form is similar to what we got in the allosteric ligand-receptor binding case, but with squared terms. The high and low ligand concentration limits are similar, except again with squared terms.

$$\text{small } c : p_{\text{active}} = \frac{1}{1 + e^{-2\beta\Delta E_u}}, \quad (6.13)$$

$$\text{large } c : p_{\text{active}} = \frac{1}{1 + \left(\frac{K_{\text{do}}}{K_{\text{dc}}} e^{-\beta\Delta E_u}\right)^2} = \frac{1}{1 + e^{-2\beta\Delta E_b}}. \quad (6.14)$$

We can thus determine the **dynamic range**,  $r$ , of the channel.

$$r = p_{\text{open}}^{\max} - p_{\text{open}}^{\min} = \frac{1}{1 + \left(\frac{K_{\text{do}}}{K_{\text{dc}}} e^{-\beta\Delta E_u}\right)^2} - \frac{1}{1 + e^{-2\beta\Delta E_u}}. \quad (6.15)$$

If we have  $N$  ion channels in a cell, the dynamic range of the entire cell is  $r_{\text{cell}} = Nr$ . The dynamic range is large for large  $\Delta E_u$  (the energy of the closed state is much higher than that of the open state in the absence of ligand) and for small  $K_{\text{do}}/K_{\text{dc}}$  (the ligands bind with much greater affinity to the open state).

### 6.2.1 The logistic equation and the Bohr parameter

The functional forms of the expressions for  $p_{\text{active}}$  in the allosteric receptor example and for  $p_{\text{open}}$  in the ligand-gated ion channel example are similar. In fact, we can re-write the functional form in terms of the logistic equation we have seen for two-state models. After all, these models are two-state models (active/inactive or open/closed); the added wrinkle is that ligand concentrations affect the probabilities of the respective states. For the ion channels, we can write

$$p_{\text{open}} = \frac{1}{1 + e^{-\beta F(c)}}, \quad (6.16)$$

a logistic equation,<sup>5</sup> where  $F(c)$  is the **Bohr parameter**.<sup>6</sup> The Bohr parameter for the ligand-gated ion channel we have been considering is

$$F(c) = 2\Delta E_u + 2k_B T \ln \left( \frac{1 + c/K_{\text{do}}}{1 + c/K_{\text{dc}}} \right). \quad (6.17)$$

Note that the Bohr parameter resembles the form of a chemical potential. The ligand-less two state model energy is adjusted by a correction related to the concentration of ligand and the respective binding energies.

### 6.2.2 Data collapse

Considering that all two-state models, including those modeled using MWC considerations, have an active (or open) probability given by the logistic equation, all  $p_{\text{active}}$  curves should fall on the same line

---

<sup>5</sup>Also called a Fermi-Dirac equation.

<sup>6</sup>The Bohr parameter is named after Christian Bohr, the father of Niels Bohr. He described what is now called the Bohr effect, in which presence of CO<sub>2</sub> decreases hemoglobin's oxygen binding efficiency. The Bohr parameter arises in that case as well.

when plotted against the Bohr parameter. So, if we could determine  $\Delta E_u$ ,  $K_{do}$ , and  $K_{dc}$  by performing experiments and statistical inference, we can compute the Bohr parameter  $F(c)$  for each value of  $c$ . If we then plot the measured  $p_{\text{active}}$  versus  $F(c)$ , all points should fall along the logistic curve given by (6.17).

To investigate this, we will use data acquired in Henry Lester's lab on the nicotinic acetylcholine receptor/ion channel. This ion channel is perhaps the best studied ion channel in nature, certainly of importance in the human nervous system. Its structure is shown in Fig. 14. The experimenters performed voltage clamp experiments to get open probabilities of the ion channels as a function of ligand (in this case acetylcholine, abbreviated ACh). They performed mutations of the different domains of the receptor and repeated the experiments, showing different responses to ligand. Their original figure is shown in Fig. 14.

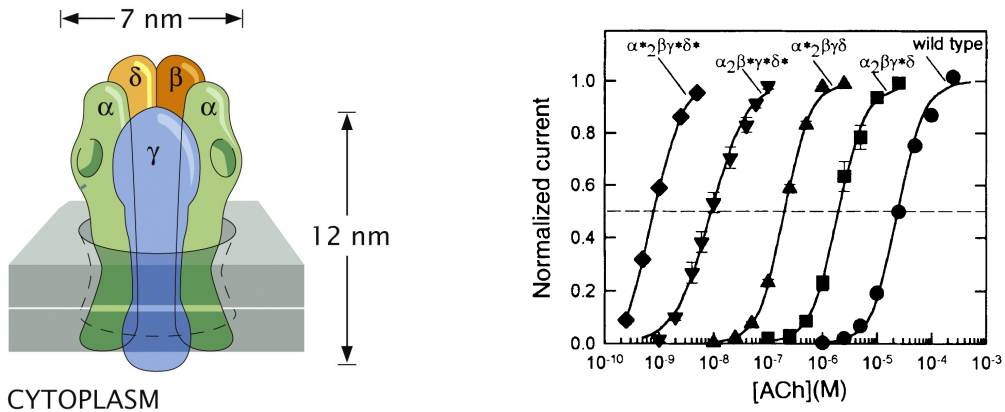


Figure 14: Left, a schematic of the nicotinic acetylcholine receptor and ion channel. Adapted from Fig. 7.26 of *PBoC2*. Right, voltage clamp experimental data for receptors containing various mutations. Figure taken from Labarca, et al., *Nature*, **376**, 514–516.

I digitized these data and performed a maximum likelihood estimate to get the necessary parameters. I then computed the Bohr parameter for each data point and plotted all data together on one plot. The result is shown in Fig. 15. The code to perform this analysis is at the end of this lecture.

### 6.2.3 Information and channel capacity

Ligand-gated ion channels sense the surroundings. If a channel is open, it is indicative that there are likely more ligands around than when it is closed. So, we may ask, how much *information* about the ligand concentration does the open or closed states of channels give the cell? Specifically, say we have  $N_{\text{cell}}$  ion channels in a cell and that  $n$  of them are open. What can we learn about the ligand concentration  $c$  given that we know  $n$  and  $N$ ?

We have already dabbled in **information theory** when we derived the Boltzmann distribution. We will now apply these ideas to quantify how much information the channel state gives about the ligand concentration. That is, we seek the **mutual information** between the open-or-closed state of the channels and the ligand concentration.

The mutual information between two random variables  $X$  and  $Y$  is the entropy loss that is incurred by knowing  $Y$ .

$$I(X; Y) = S[X] - S[X | Y], \quad (6.18)$$

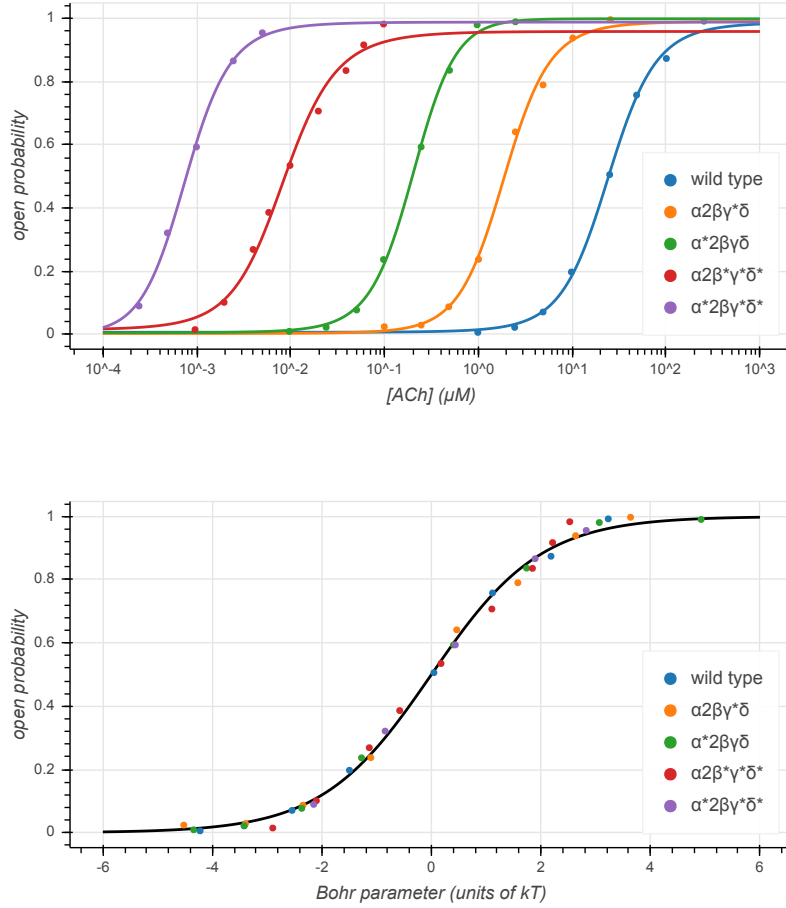


Figure 15: Top, results of maximum likelihood estimate curve fits of the data from Labarca, et al., *Nature*, 376, 514–516. Bottom, all data sets plotted against the Bohr parameter. The logistic curve is shown in black.

where we have introduced the notion of **conditional entropy**,

$$S[X \mid Y] = \sum_y P(y) \left( - \sum_x P(x \mid y) \log_2 P(x \mid y) \right). \quad (6.19)$$

The conditional entropy is then the entropy associated with the distribution  $P(X \mid Y)$ , averaged over  $Y$ . The mutual information is then

$$I(X; Y) = - \sum_x P(x) \log_2 P(x) + \sum_y P(y) \left( \sum_x P(x \mid y) \log_2 P(x \mid y) \right). \quad (6.20)$$

It can be shown that the mutual information is symmetric, such that  $I(X; Y) = I(Y; X)$ .

In the present case, we take  $X = c$  and  $Y = n$ . I will not work out the mathematical details here (see the [Marzen and Phillips paper](#)), but will state without proof that the maximum mutual information possible, called the **channel capacity**, is approximately (in the low noise limit)

$$I_{\text{opt}} \approx \log_2 \left( \frac{1}{\sqrt{2\pi e}} \int dn \sigma_n \right), \quad (6.21)$$

where  $\sigma_n$  is the standard deviation of  $P(n \mid c, N)$ . We know that  $P(n \mid c, N)$  describes a Binomial distribution, where the probability that a given channel is open is given the expression we derived in (6.8). The standard deviation is then that for a Binomial distribution,

$$\sigma_n^2 = N p_{\text{open}} (1 - p_{\text{open}}). \quad (6.22)$$

Using this expression and evaluating the integral gives

$$I_{\text{opt}} \approx \log_2 \left( \sqrt{\frac{2N}{\pi e}} \left( \sin^{-1} \sqrt{p_{\text{open}}^{\max}} - \sin^{-1} \sqrt{p_{\text{open}}^{\min}} \right) \right), \quad (6.23)$$

which is related to the dynamic range, since the inverse sine function  $\sin^{-1}(x)$  is monotonic on the interval  $0 \leq x \leq 1$ .

So, the bigger the dynamic range, the larger the channel capacity, and the more then cell and “know” about its surroundings. As we have seen, having multiple ligands bind to the channel to control the gating where binding it tighter when the channel is open, boosts the dynamic range, therefore increasing the channel capacity.

```

1 import numpy as np
2 import pandas as pd
3 import scipy.optimize
4 import bokeh.plotting
5 import bokeh.io

6
7 # Load in data set
8 df = pd.read_csv('lester_acetylcholine.csv')

9
10 # Get units in molar
11 df[['ACh] (M)']] *= 1e6

12 df = df.rename(columns={'[ACh] (M)': '[ACh] (\mu M)'})

13
14 # Set up data frame with MLE results
15 cols = ['Kd_open', 'Kd_closed', 'beta_deltaE', 'genotype']
16 df_best_fit = pd.DataFrame(columns=cols)

17
18
19
20 def p_open_theor(c, log_Kd_open, log_Kd_closed, beta_deltaE):
21     """Theoretical curve for open probability"""
22     Kd_open = np.exp(log_Kd_open)
23     Kd_closed = np.exp(log_Kd_closed)
24     a = (1 + c/Kd_open)**2
25     b = (1 + c/Kd_closed)**2

26     return a / (a + b * np.exp(-beta_deltaE))

27
28
29
30 def resid(params, c, p_open):
31     """Residual from theoretical for use in least squares."""
32     return p_open - p_open_theor(c, *params)

33
34

```

```

35 # Set up plots
36 p = bokeh.plotting.figure(plot_height=300,
37                           plot_width=600,
38                           x_axis_label='[ACh] ( $\mu$ M)',
39                           y_axis_label='open probability',
40                           x_axis_type='log')
41 p2 = bokeh.plotting.figure(plot_height=300,
42                           plot_width=600,
43                           x_axis_label='Bohr parameter (units of kT)'
44                           ,
45                           y_axis_label='open probability')
46
47 # Theoretical logistic curve
48 F = np.linspace(-6, 6, 200)
49 p2.line(F, 1 / (1 + np.exp(-F)), color='black', line_width=2)
50
51 colors = bokeh.palettes.d3['Category10'][10]
52 Ach_smooth = np.logspace(-4, 3, 200)
53
54 # Initial guess for curve fits
55 p0 = np.array([-1, 0, -6])
56
57 for i, gtype in enumerate(df['genotype'].unique()):
58     # Load in data for one genotype
59     sub_df = df.loc[df['genotype']==gtype, :]
60     c, p_open = sub_df['[ACh] ( $\mu$ M)'].values, sub_df['p_open'].values
61
62     # Perform curve fit
63     res = scipy.optimize.least_squares(resid, p0, args=(c, p_open))
64
65     # Store results
66     Kd_open, Kd_closed = np.exp(res.x[:2])
67     beta_deltaE = res.x[2]
68     df_res = pd.DataFrame(columns=cols,
69                           data=[[Kd_open, Kd_closed, beta_deltaE,
70 gtype]])
71     df_best_fit = df_best_fit.append(df_res, ignore_index=True)
72
73     # Plot fits
74     p.line(Ach_smooth,
75            p_open_theor(Ach_smooth, *res.x),
76            line_width=2,
77            color=colors[i])
78     p.circle(c, p_open, color=colors[i], legend=gtype)
79
80     # Plot using Bohr parameter (data collapse)
81     a = (1 + c/Kd_open)**2
82     b = (1 + c/Kd_closed)**2
83     F = beta_deltaE + np.log(a) - np.log(b)
84     p2.circle(F, p_open, color=colors[i], legend=gtype)

```

```
85 p.legend.location = 'bottom_right'  
86 p2.legend.location = 'bottom_right'  
87  
88 # Save as SVG  
89 p.output_backend = 'svg'  
90 p2.output_backend = 'svg'  
91 bokeh.io.export_svgs(p, filename='lester_mle.svg')  
92 bokeh.io.export_svgs(p2, filename='lester_dataCollapse.svg')
```

lester\_curves.py

# 7 Statistical mechanics of gene expression regulation

We have been using the tools of statistical mechanics, and two-state and MWC models in particular, to study a host of problems, including ligand-receptor binding, allostery, operation of ion channels, and even single molecule experiments in the homework. We will now use the tools of statistical mechanics to study the regulation of **gene expression**. A gene is **expressed** when its gene product is produced by the cell, first by transcription of mRNA by RNA polymerase and then translation of the mRNA into protein by the ribosomes. As in the previous applications of statistical mechanics, the power of this approach lies in

- The ease of mathematizing cartoons using states and weights.
- Dissociation constants emerge, and these can be *measured*.
- Allows identification of the “knobs” that can be used to tune gene expression.

## 7.1 Gene expression preliminaries

To begin talking about regulation of gene expression, we need to first understand the basic architecture of a gene. We will focus on bacteria; eukaryotic gene architecture is typically more complex.

Fig. 16 show a cartoon of the promoter region of a gene. The colored rectangle represents the DNA. The light pink region to the right is the start of the coding region of the gene. Ahead of the gene is a **promoter**, which is the part of the DNA that the **RNA polymerase** binds to to start transcription. The promoter region is decorated with binding sites for other molecules generically termed **transcription factors**.

An activating transcription factor, or **activator**, may bind a region near the promoter, and then can have a favorable interaction with the polymerase. As we will see when we work out the statistical mechanics, this results in recruiting more polymerase to the promoter and therefore gives higher expression of the gene.

A repressive transcription factor, or **repressor**, may bind to a part of the promoter region, sometimes called an **operator**. When it does so, it occludes or otherwise inhibits the polymerase from binding the promoter.

It is useful to know some typical numbers about this system.

quantity	value	BNID
RNA polymerase footprint	≈ 40 base pairs	<a href="#">107873</a>
elongation rate	≈ 60 nucleotides/second	<a href="#">103021</a>
initiation rate	≈ 20 transcripts/minute	<a href="#">111997</a>
number of RNA polymerases per cell	≈ 1000	<a href="#">101440</a>

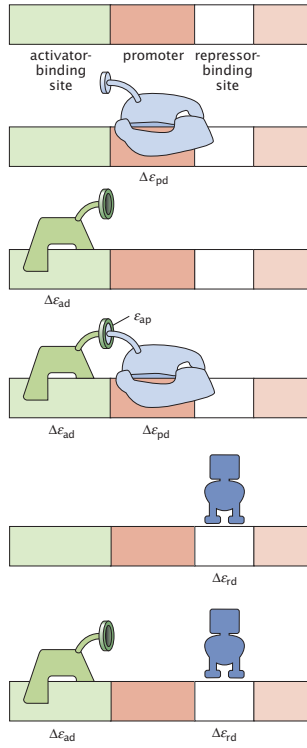


Figure 16: A sketch of the promoter region of a gene. The RNA polymerase (light blue) binds to the promoter to start transcription. It is occluded from doing so when a repressor is bound to the repressor binding site. If an activator is bound to the activated binding site, the polymerase has a favorable interaction with it when bound to the promoter. This figure is adapted from *PBoC2* Fig. 19.18. In *PBoC2*, the energies are denoted with  $\epsilon$ 's; we will use  $E$ 's.

## 7.2 Separation of time scales

In our modeling, we will assume that the *rate* of production of mRNA transcripts for a particular gene is proportional to the *equilibrium* probability that a polymerase molecule is bound to the promoter of the gene. This seems odd at first glance, that we would use an equilibrium thermodynamic property,  $p_{\text{bound}}$ , to describe a kinetic process, the rate of production. The key to this assumption being valid is a **separation of time scales** in the transcription process.

Getting the polymerase started is inefficient. The polymerase tends to bind and rebinding to the promoter. It often generates small transcripts that are disregarded, and then rebinds and starts over. Typically after many binding and unbinding events, the polymerase gets going with transcription. The binding and unbinding of the polymerase to the promoter is very fast, so fast that it is typically not measurable. The dissociation constant, however, can be measured, and can be as small as  $K_d = 5 \text{ nM}$  ([BNID 103592](#)).

We can write the reaction scheme of a polymerase getting started making a transcript as



Using mass action kinetics, we can write the dynamical equations of the unbound (u), bound (b), and

elongating (e) states as

$$\frac{dP_u}{dt} = -k_+ P_u c_p + k_- P_b \quad (7.2)$$

$$\frac{dP_b}{dt} = k_+ P_u c_p - k_- P_b - \alpha_m P_b, \quad (7.3)$$

$$\frac{dP_e}{dt} = \alpha_m P_b, \quad (7.4)$$

where  $P_i$  is the probability of being in state  $i$  and  $c_p$  is the concentration of available polymerase. If we define the dimensionless time  $\tau = k_- t$ , the equations are

$$\frac{dP_u}{d\tau} = -P_u c_p / K_d + P_b \quad (7.5)$$

$$\frac{dP_b}{d\tau} = P_u c_p / K_d - P_b - \frac{\alpha_m}{k_-} P_b, \quad (7.6)$$

$$\frac{dP_e}{d\tau} = \frac{\alpha_m}{k_-} P_b, \quad (7.7)$$

where we have defined  $K_d = k_- / k_+$ . In looking at the above, if  $\alpha_m / k_- \ll 1$ , then the dynamics of the second ODE (7.6) are much slower than the first (7.5). The probability  $P_u$  rapidly comes to steady state, so

$$\frac{dP_u}{d\tau} = -P_u c_p / K_d + P_b \approx 0. \quad (7.8)$$

So,  $P_b$  is entirely determined from this equation, which is in fact an equilibrium equation. The last equation, (7.7), then states that the rate of elongation, which is the rate of production of mRNA transcripts, is proportional to the *equilibrium* probability of the promoter being bound,  $P_b$ .

So, our goal in quantifying the rate of production of mRNA for a target gene is to compute the probability that the polymerase is bound to the promoter at equilibrium. The statistical mechanical approach we have developed are well suited for this task.

### 7.3 Statistical mechanics of unregulated gene expression

Let us now consider computing  $P_b$  for the case where the expression is unregulated. That is, there are no repressors or activators. There are then two states to consider, the promoter is bound or the promoter is unbound. Let's write a states and weights table.

state	statistical weight
unbound	$e^{-\beta E_u}$
bound	$e^{-\beta(E_b - \mu_p)}$

Here, we have done what we did in past lectures, subtracting a chemical potential of the polymerase to keep track of the loss of entropic degrees of freedom when it binds the promoter. But what is the chemical potential of the unbound polymerase,  $\mu_p$ ? We need to think a bit more carefully about this.

It is important to know that nearly all polymerases are bound to the genome and plasmids. This is known from experiments where cells divide asymmetrically and the DNA-less cell has virtually no polymerases. So, all of the polymerases are bound to the DNA. They are just bound nonspecifically.

Let  $P$  be the number of polymerases that are available to transcribe the gene of interest.<sup>7</sup> Let  $N_{\text{NS}}$  be the number of nonspecific sites on the genome to which a polymerase can bind. Since the *E. coli* genome is about  $4 \times 10^6$  base pairs, and there are only about 1000 polymerases per cell, and each polymerase is about 40 base pairs across,  $N_{\text{NS}}/P \approx 100$  as a lower bound<sup>8</sup>, and we will take  $N_{\text{NS}} \gg P$ .

With this in mind, we can rewrite the states and weights table explicitly taking into account the multiplicity of states.

state	statistical weight
unbound	$\frac{N_{\text{NS}}!}{P!(N_{\text{NS}}-P)!} e^{-\beta PE_{\text{pd}}^{\text{NS}}}$
bound	$\frac{N_{\text{NS}}!}{(P-1)!(N_{\text{NS}}-P+1)!} e^{-\beta(P-1)E_{\text{pd}}^{\text{NS}}} e^{-\beta E_{\text{pd}}^{\text{S}}}$

Here,  $E_{\text{pd}}^{\text{NS}}$  denotes the energy of nonspecific binding of the polymerase to DNA, and  $E_{\text{pd}}^{\text{S}}$  denotes the energy of specific binding of the polymerase to DNA. If  $N_{\text{NS}} \gg P$ , then

$$\frac{N_{\text{NS}}!}{(N_{\text{NS}} - P)!} \approx (N_{\text{NS}})^P. \quad (7.9)$$

With this approximation, we can write  $P_b$  as

$$P_b = \frac{\frac{N_{\text{NS}}^{P-1}}{(P-1)!} e^{-\beta(E_{\text{pd}}^{\text{S}} + (P-1)E_{\text{pd}}^{\text{NS}})}}{\frac{N_{\text{NS}}^{P-1}}{(P-1)!} e^{-\beta(E_{\text{pd}}^{\text{S}} + (P-1)E_{\text{pd}}^{\text{NS}})} + \frac{(N_{\text{NS}})^P}{P!} e^{-\beta PE_{\text{pd}}^{\text{NS}}}}. \quad (7.10)$$

Dividing top and bottom by the last term in the denominator yields

$$P_b = \frac{\frac{P}{N_{\text{NS}}} e^{-\beta \Delta E_{\text{pd}}}}{1 + \frac{P}{N_{\text{NS}}} e^{-\beta \Delta E_{\text{pd}}}}, \quad (7.11)$$

where  $\Delta E_{\text{pd}} = E_{\text{pd}}^{\text{S}} - E_{\text{pd}}^{\text{NS}}$  is the difference in energy between specific and nonspecific binding. Typically,  $\Delta E_{\text{pd}} < 0$ .

In looking at this expression, it is clear that our  $\mu$  in our original states and weights table on page 47 is

$$\mu_p = E_{\text{pd}}^{\text{NS}} + k_B T \ln \frac{P}{N_{\text{NS}}}. \quad (7.12)$$

This is the same form as the chemical potential of ligands in a dilute solution, with the mole fraction replaced by  $P/N_{\text{NS}}$ . With this convention, we also find that the statistical weight associated with the unbound state is unity. The states and weights table is then conveniently written as

---

<sup>7</sup>Some of the cell's polymerases may be transcribing genes or are bound to other promoters. We will take  $P$  to be all of those available with the correct  $\sigma$  factor.

<sup>8</sup>The ratio is even bigger, since we could consider each one-base shift to be another non-specific binding site.

state	statistical weight
unbound	1
bound	$e^{-\beta(E_{pd}^S - \mu_p)} = \frac{P}{N_{NS}} e^{-\beta\Delta E_{pd}}$ .

Because it comes up so often, for convenience going forward, we define

$$\rho = \frac{P}{N_{NS}} e^{-\beta\Delta E_{pd}}, \quad (7.13)$$

such that the probability that an unregulated promoter is bound is  $P_b = \rho / (1 + \rho)$ .

## 7.4 Simple repression

Now, we will consider the case where a repressor can bind to the promoter region and occlude the polymerase from binding. As we write our states and weights table, we are again faced with how to write a chemical potential, this time for repressors. In fact, most repressors are also bound to DNA, either specifically or nonspecifically. We can see this by considering that the dissociation constant for nonspecific binding of repressors to DNA is about  $10 \mu M$ .<sup>9</sup> The number of nonspecific binding sites, accounting for possible overlap, is about  $10^5$  per cell, for a concentration of about  $200 \mu M$ . The equilibrium expression for receptor-nonspecific site binding is

$$K_d = \frac{c_{NS} c_R^0}{c_{R-NS}} = \frac{(c_{NS} - c_{R-NS})(c_R^0 - c_{R-NS})}{c_{R-NS}} \approx \frac{c_{NS}^0 (c_R^0 - c_{R-NS})}{c_{R-NS}}. \quad (7.14)$$

In the last approximation, we have used that fact that there are far fewer repressors than nonspecific binding sites, since repressor copy numbers range from 10 to 10,000 per cell ([BNID 102632](#)). We can rearrange this to get

$$c_{R-NS} = \frac{c_R^0 c_{NS}^0}{K_d + C_{NS}^0} = \frac{c_R^0}{1 + K_d/c_{NS}^0}. \quad (7.15)$$

Because  $K_d \ll c_{NS}^0$ , we have  $c_{R-NS} \approx c_R^0$ , so nearly all repressors are bound to DNA.

We therefore know that the chemical potential term in the states and weights table for repressors is  $\mu_r = E_{rd}^S + k_B T \ln R/N_{NS}$ . So, our states and weights table for repressor-mediated transcription is

state	statistical weight
unbound	1
polymrerase bound	$\rho$
repressor bound	$e^{-\beta(E_{rd}^S - \mu_r)} = \frac{R}{N_{SS}} e^{-\beta\Delta E_{rd}}$

From the states and weights table, we get

$$P_b = \frac{\rho}{1 + \rho + \frac{R}{N_{SS}} e^{-\beta\Delta E_{rd}}}. \quad (7.16)$$

<sup>9</sup>I got this number from [Bintu, et al., Curr. Op. Genet. Dev., 15, 116–124, 2005](#).

### 7.4.1 Fold change

A more convenient metric to measure experimentally is the **fold change** in gene expression, defined as

$$\text{fold change} = \frac{P_b}{P_b(R=0)}. \quad (7.17)$$

The unregulated probability of bound polymerase is always  $\rho/(1+\rho)$ , so it is convenient to write

$$P_b = \frac{\rho}{1+\rho} (\text{fold change}) = \frac{\rho}{1+\rho} \frac{1}{1 + \frac{R}{(1+\rho)N_{\text{ss}}} e^{-\beta \Delta E_{\text{rd}}}} \quad (7.18)$$

The fold change is then

$$\text{fold change} = \frac{1}{1 + \frac{R}{(1+\rho)N_{\text{ss}}} e^{-\beta \Delta E_{\text{rd}}}}. \quad (7.19)$$

The value of  $\rho$  will vary from promoter to promoter. The term  $P/N_{\text{NS}}$  is close to the same for all bacterial cells, with

$$\frac{P}{N_{\text{NS}}} \approx \frac{10^3}{10^6} \approx 10^{-3}. \quad (7.20)$$

For the lac promoter,  $\Delta E_{\text{pd}} \approx -3k_B T$ , and for the T7 promoter, which codes for the protein of the T7 phage,  $\Delta E_{\text{pd}} \approx -8k_B T$ . Thus, for lac,  $\rho \approx 10^{-2}$ , and for T7,  $\rho \approx 1$ . For the former case,  $\rho$  is small, and we have a **weak promoter**. A weak promoter allows for easier regulation; it takes less repressors to see a change in expression levels, since for weak promoters,

$$\text{fold change} \approx \frac{1}{1 + \frac{R}{N_{\text{ss}}} e^{-\beta \Delta E_{\text{rd}}}}. \quad (7.21)$$

In this form, we see that the quantity  $N_{\text{NS}} e^{\beta \Delta E_{\text{rd}}}$  is akin to a dissociation constant in ligand-receptor binding. Defining  $K_r \equiv N_{\text{NS}} e^{\beta \Delta E_{\text{rd}}}$ , we can write the fold change as

$$\text{fold change} \approx \frac{1}{1 + R/K_r}. \quad (7.22)$$

A cell can tune  $R$  by regulating the expression of the repressor itself, and evolution can tune  $\Delta E_{\text{rd}}$ .

## 7.5 Simple activation

Let us now turn our attention to simple activation. In this case, there is no repressor; just an activator that has a favorable interaction with the polymerase. We can again write our states and weights, and can do so taking shortcuts we have already worked out. Specifically, we know that it is always the *difference* in energy between specific and nonspecific binding that comes into the statistical weights. We also know that most activators, like repressors, are bound to promoter regions or to nonspecific sites on the DNA. The only added wrinkle in this example is the extra energy,  $\Delta E_{\text{pa}}$ , in the state where both the activator and polymerase are bound that is due to the favorable interaction between the activator and polymerase.

state	statistical weight
unbound	1
polymerase bound	$\rho$
activator bound	$\frac{A}{N_{SS}} e^{-\beta \Delta E_{ad}}$
activator and polymerase bound	$\rho \frac{A}{N_{SS}} e^{-\beta (\Delta E_{ad} + \Delta E_{pa})}$

The numerator in the expression for  $P_b$  contains the weights where the polymerase is bound, in this case two of entries from the states and weights table.

$$\begin{aligned}
 P_b &= \frac{\rho + \rho \frac{A}{N_{SS}} e^{-\beta (\Delta E_{ad} + \Delta E_{pa})}}{1 + \rho + \frac{A}{N_{SS}} e^{-\beta \Delta E_{ad}} + \rho \frac{A}{N_{SS}} e^{-\beta (\Delta E_{ad} + \Delta E_{pa})}} \\
 &= \frac{\rho}{1 + \rho} \frac{1 + \frac{A}{N_{SS}} e^{-\beta (\Delta E_{ad} + \Delta E_{pa})}}{1 + \frac{A}{(1+\rho)N_{SS}} e^{-\beta \Delta E_{ad}} + \rho \frac{A}{(1+\rho)N_{SS}} e^{-\beta (\Delta E_{ad} + \Delta E_{pa})}} \\
 &= \frac{\rho}{1 + \rho} \frac{1 + (A/K_{d,a})e^{-\beta \Delta E_{pa}}}{1 + A/K_{d,a} + \frac{\rho}{1+\rho} (A/K_{d,a})e^{-\beta \Delta E_{pa}}}. \tag{7.23}
 \end{aligned}$$

Here, we have defined  $K_{d,a}$  analogously to  $K_{d,r}$  from before,

$$K_{d,a} = N_{SS} e^{\beta \Delta E_{ad}}. \tag{7.24}$$

This is the dissociation constant activator binding to the promoter region.

We can immediately extract the expression for the fold change,

$$\text{fold change} = \frac{1 + (A/K_{d,a})e^{-\beta \Delta E_{pa}}}{1 + A/K_{d,a} + \frac{\rho}{1+\rho} (A/K_{d,a})e^{-\beta \Delta E_{pa}}}. \tag{7.25}$$

The fold change can actually be less than one if the promoter is strong (or if  $\Delta E_{pa}$  is large and positive). That means that presence of the activator can actually decrease expression. If we want good control of expression by an activator, then, we need to have a favorable interaction between the polymerase and the activator ( $\Delta E_{pa} < 0$ ) and a weak promoter ( $\rho \ll 1$ ). Provided this is the case, such that  $\rho/(1 + \rho) \approx \rho \ll 1$ , the maximum possible fold change can be found by taking the limit of large  $A$ . We get a maximum fold change of  $e^{-\Delta E_{pa}}$ .

## 7.6 Cooperative repression

Now imagine a situation where two repressors can bind to the operator. We may get additional energetic contribution if there are two repressors,<sup>10</sup> say  $\Delta E_{rr}$ . We can again directly write the states and weights table.

---

<sup>10</sup> *PBoC2* uses the notation  $\Delta E_{rr} = J$ .

state	statistical weight
unbound	1
polymerase bound	$\rho$
one repressor bound	$2R/K_{d,r}$
two repressors bound	$(R/K_{d,r})^2 e^{-\beta \Delta E_{rr}}$

The probability of having the polymerase bound is then

$$P_b = \frac{\rho}{1 + \rho} \frac{1}{1 + \frac{1}{1+\rho}(R/K_{d,r})(2 + (R/K_{d,r})e^{-\beta \Delta E_{rr}})}. \quad (7.26)$$

For a weak promoter, this reduces to

$$\begin{aligned} P_b &= \frac{\rho}{1 + \rho} \frac{1}{1 + (R/K_{d,r})(2 + (R/K_{d,r})e^{-\beta \Delta E_{rr}})} \\ &= \frac{\rho}{1 + \rho} \frac{1}{(1 + R/K_{d,r})^2 + (e^{-\beta \Delta E_{rr}} - 1)(R/K_{d,r})^2}. \end{aligned} \quad (7.27)$$

The case where there is no enhanced binding of the second receptor, i.e.,  $\Delta E_{rr} = 0$ , reduces to

$$P_b = \frac{\rho}{1 + \rho} \frac{1}{(1 + R/K_{d,r})^2}. \quad (7.28)$$

So, cooperative binding, with  $\Delta E_{rr} < 0$ , gives greater repression than without cooperative binding.

The analyses in this lecture demonstrate how carefully considering the statistical mechanics of gene expression reveals what parameters, usually energetics of binding interactions, may be adjusted to tune the properties of regulation of gene expression.